Table 1. Primers for Real-Time RT-PCR

Gene		Sequence	Product size (bp)	Accession number
β-actin	Forward	5′-AAGTACCCCATTGAACACGG-3′	257	NM_031144
	Reverse	5′-ATCACAATGCCAGTGGTACG-3′		
MMP-2	Forward	5′-GATGGCAAGGTGTGGTGTG-3′	191	NM_031054
	Reverse	5′-AATCGGAAGTTCTTGGTGTAGG-3′		
MMP-3	Forward	5′-TGGCAGTGAAGAAGATGCTG-3′	167	NM_133523
	Reverse	5′-GCTTCCCTGTCATCTTCAGC-3′		
MMP-9	Forward	5′-CGCTTGGATAACGAGTTCTCTC-3′	163	NM_031055
	Reverse	5′-GCAGGAGGTCATAGGTCACG-3′		
MMP-10	Forward	5′-ACCCCACTCACATTCTCCAG-3′	163	NM_133514
	Reverse	5′-CATCGAAGTGAGCATCTCCA-3′		
MMP-13	Forward	5′-GCACTACTTGAAATCATACTACCATCC-3′	183	NM_133530
	Reverse	5′-ACATCAGGCACTCCACATCTTG-3′		
MMP-14	Forward	5′-AGTCAGGGTCACCCACAAAG-3′	204	NM_031056
	Reverse	5′-GGTATCCGTCCATCACTTGG-3′		
VEGF	Forward	5′-CTACCTCCACCATGCCAAGT-3′	183	NM_031836
	Reverse	5′-ACACAGGACGGCTTGAAGAT-3′		
CXCR4	Forward	5′-TCCGTGGCTGACCTCCTCTT-3′	210	NM_022205
	Reverse	5′-CAGCTTCCTCGGCCTCTGGC-3′		

master SYBR Green I (Roche Diagnostics, Pleasanton, CA) in Light Cycler (Roche Diagnostics). The design of the oligonucleotide primers was based on published rat cDNA sequences. When rat sequences were not available, porcine sequences were used. The RT-PCR products were subcloned into pGEM-T Easy vector (Promega, Madison, WI) and confirmed by sequencing based on published cDNA sequences. Expression in the pulp tissue immediately, and 12, 24, 48, and 72 hours after injury, was compared with rat normal pulp tissue after normalizing with β-actin. The experiments were repeated three times, and one represented experiment is presented.

Immunohistochemistry

For double-staining immunohistochemistry of CXCR4 and MMP-3, cryotome sections (12 μm thick) of 24 and 72 hours after injury were used. The endogenous peroxidase activity was blocked with 2% hydrogen peroxide in methanol for 20 minutes. To avoid nonspecific staining, the sections were incubated with 10 mg/ml blocking reagent (PerkinElmer, Boston, MA) for 1 hour at room temperature and then reacted with goat anti-CXCR4 (1/50) in Canget 1 buffer (Toyobo) for 1 hour at room temperature. After three washes in PBT (PBS, 0.05% Tween 20, pH 7.4), sections were incubated with rabbit anti-goat IgG Alexa 488 (1/200) in PBT for 1 hour at room temperature. Unbound antibodies were washed three times with PBT. Sections were incubated with mouse anti-MMP-3 (0.5 μg/ml) in Canget 1 buffer overnight at 4°C. After three washes in PBT, bound antibodies were reacted with a horseradish peroxidase-labeled goat anti-mouse IgG secondary antibody for 1 hour at room temperature. Color was developed using tyramide signal amplification system Rhodamine-conjugated tyramide (Invitrogen) according to the manufacturer's instructions. All slides were developed in parallel, and the reaction was stopped before detection of nonspecific staining in control preimmune serum-treated sections. Sections were then stained with dye Hoechst 33342 (Sigma) and mounted with Prolong Gold antifade reagent (Invitrogen) and photographed on a Zeiss Confocal LSM510 microscope (Carl Zeiss, Berlin, Germany). To confirm the localization of MMP-3 in blood vessels, frozen sections were treated with 20 μg/ml proteinase K (Invitrogen) for 6 minutes at room temperature. After three washes in PBS, sections were stained with 20 μg/ml Fluorescein Griffonia (Bandeiraea) Simplicifolia lectin (BS1-lectin) (Vector Laboratories, Burlingame, CA) for 15 minutes. This BS1-lectin has been used for specific staining of endothelial cells and endothelial progenitor cells.[24] After three washes in PBS, sections were stained with MMP-3 as described above. As negative controls, both only primary antibodies and only secondary antibodies were used. Normal mouse IgG was also used for determination of nonspecific binding of anti-mouse MMP-3 antibody.

In Situ *Hybridization Analysis*

In situ hybridization staining of sections was done as described previously.[25] The cryotome sections obtained 24 and 72 hours after injury were observed by *in situ* hybridization analysis using a rat MMP-3 anti-sense probe. The probes were constructed out of the plasmids after subcloning the PCR product using the same primers designed for real-time RT-PCR (Table 1).

Proliferation, Migration, and Antiapoptosis Analysis

For proliferation analysis, human umbilical vein endothelial cells (HUVECs) (KURABO Industries, Osaka, Japan) at third passage were seeded with 1000 cells per 96-well. They were cultured in endothelial basal medium-2 in the presence of human MMP-3 (50 ng/ml; Chemicon, Temecula, CA) with or without *N*-Isobutyl-*N*-(4-methoxyphenylsulfonyl)-glycylhydroxamic acid (NNGH) (0.13 μmol/L; Biomol, Plymouth Meeting, PA), NNGH only, MMP-10 (50 ng/ml; R&D Systems, Minneapolis, MN), or VEGF-A (50 ng/ml; PeproTech, London, UK). NNGH is highly specific for MMP-3 at the concentration used.[26] Ten microliters of Tetra-color one

(Seikagaku Kogyo, Tokyo, Japan) was added to the 96-well plate, and cell numbers were measured using spectrophotometer at 450 nm absorbance at 2, 12, 24, 36, 48, and 60 hours of culture. As a control, cells were cultured without any supplement. Wells without cells were served as negative controls.

For migration analysis, modified Boyden chamber assays were performed for 24 hours at 37°C with polyethylene terepthlate membrane (BD Biosciences, Franklin Lakes, NJ) in 24-well plates. In brief, HUVECs (10,000/well) were cultured in the upper chamber in the presence of 10 or 100 ng/ml MMP-3 with or without 0.13 μmol/L NNGH, 50 ng/ml MMP-10 with or without 0.13 μmol/L NNGH, NNGH only, or 50 ng/ml VEGF-A. As a control, 0.2% bovine serum albumin (Sigma) was used. After the incubation period, the migrated HUVECs attached to the lower side of the filter were harvested by trypsinization and counted. The numbers of migrated cells were enumerated. The nonmigrated cells on the upper side of the filter were scraped off with a rubber scraper.

To evaluate the effect of MMP-3 on anti-apoptosis, HUVEC at passage 6 or less were grown in endothelial growth medium-2 in a 35-mm dish for 3 days and then incubated with 100 nmol/L staurosporine (Sigma) in EBM-2 supplemented with 50 ng/ml MMP-3 with or without 0.13 μmol/L NNGH, NNGH only, 50 ng/ml MMP-10, or VEGF-A. NNGH was added 30 minutes before adding MMP-3. As a control, cells were cultured in EBM-2 without any supplement in the presence of staurosporine. After 4 hours, HUVECs were harvested, and the cell suspensions were stained with Annexin V-FITC (Roche) and propidium iodide (Roche) for 15 minutes and then ana-

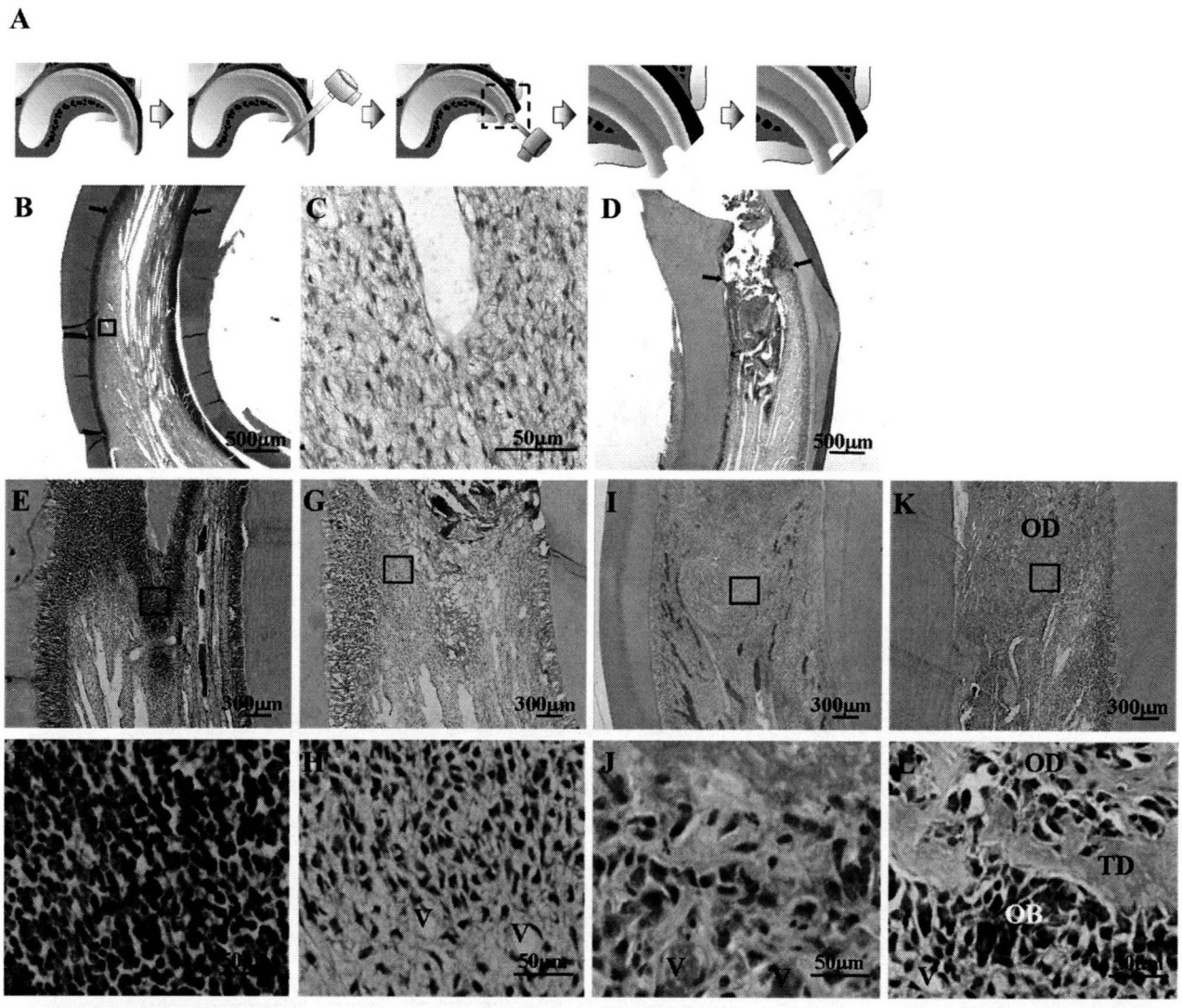

Figure 1. Morphological analysis by H&E staining of wound-healing process in rat-injured pulp. **A:** Schematic diagrams of amputation and filling of rat upper incisor. **Left** to **right:** rat upper incisor, removing the upper part of crown with a diamond point burr, amputation of pulp with a round burr, washing and stop bleeding, and filling with spongel and resin. **B:** Low power normal pulp. **Arrows** indicate imaginary amputated site. **C:** High power normal pulp; from the boxed area in **B**. **D:** A lower power image of the wound-healing event under the amputated site (**arrows**) at 12 hours after injury. **E** and **F:** One hour after injury, hyperemia, dilatation of blood vessels, and infiltration of neutrophils were observed in upper part of pulp tissue under the amputated site. Twenty-four hours after injury, no inflammatory cells were found, and the denatured tissue was seen under the amputated site. **G** and **H:** A large number of polygonal-shaped cells in pulp can be observed. **I** and **J:** Seventy-two hours after injury, spindle-shaped cells were embedded in collagenenous matrix. **K** and **L:** Seven days after injury, odontoblast-like cells and tubular dentin are seen. OD, osteodentin; V, newly formed blood vessels; OB, odontoblast-like cells; TD, tubular dentin. The **upper panels** (**E**, **G**, **I**, **K**) represent the amputated site. The lower panels (**F**, **H**, **J**, **L**) are magnified from the corresponding boxes in the panel above.

lyzed by flow cytometry (Bay bioscience, Kobe, Japan). The experiments were repeated three times, and one represented experiment is presented.

MMP-3 Protein Application on the Amputated Pulp

After amputation of rat incisor pulp as described above, 50 ng of MMP-3 absorbed in spongel was applied on the amputated pulp. As controls, PBS absorbed in spongel or NNGH together with MMP-3 was used. The cavities were filled with the bonding agent and resin as described above. The paraffin sections (5-μm thickness) of 24 hours, 72 hours, and 7 days after treatment were morphologically examined after H&E staining or Masson trichrome staining.

For quantitative analysis of newly formed blood vessels, each five frozen sections at 24 hours after treatment, both with MMP-3 and control PBS from four incisors each, a total of 40 sections were stained with Fluorescein Griffonia (Bandeiraea) Simplicifolia lectin (BS1-lectin) as described above. Three rectangles of a standardized size (0.1 mm^2) were drawn in the upper part of pulp tissue under the amputated site in every five sections from one sample. The lectin-positive area relative to total area (1.5 mm^2) was quantitatively analyzed in a standardized procedure using BZ-II Analyzer (Keyence, Tokyo, Japan) software on a Keyence BZ-9000 fluorescence microscope (Keyence). The data were presented as means ± SD at four determinations.

To evaluate effect of MMP-3 on proliferation, immunohistochemical analysis of PCNA was performed. Paraffin sections of 24 hours after treatment were deparaffinized, and antigen was retrieved by antigen unmasking solution (Vector Laboratories), according to the manufacturer's instructions. Endogenous peroxidase activity and nonspecific staining were blocked as described earlier. The sections were incubated with anti-PCNA antibody (Dako) at dilutions of 1/100 in antibody diluent (Dako) overnight at 4°C and further incubated with a peroxidase-conjugated secondary antibody (ImmPRESS reagent; Vector Laboratories) for 30 minutes at room temperature. After development by DAB+Liquid System (Dako), sections were counterstained with hematoxylin and photographed on an Olympus Vanox-s microscope (Olympus, Tokyo, Japan). For quantitative analysis of proliferating cells, each three paraffin sections at 24 hours after treatment, both with MMP-3 and control PBS from 4 incisors each, were used. Three rectangles of a standardized size (0.1 mm^2) were drawn in the upper part of pulp tissue under the amputated site in every three sections. The positive staining cells were counted and quantitatively analyzed. The data were presented as means ± SD at four determinations.

For quantitative analysis of matrix formation, three fields of each five paraffin sections at 72 hours after treatment, both with MMP-3 and control PBS from four incisors each, and three fields of five sections at 7 days after treatment with MMP-3, MMP-3+NNGH, PBS+NNGH, and control PBS from four incisors each were stained with Masson trichrome staining. The positive area was quantitatively analyzed in the upper part of pulp tissue under the amputated site, 2 mm in depth from the amputated site, using BZ-II Analyzer software. The data were presented as means ± SD at four determinations.

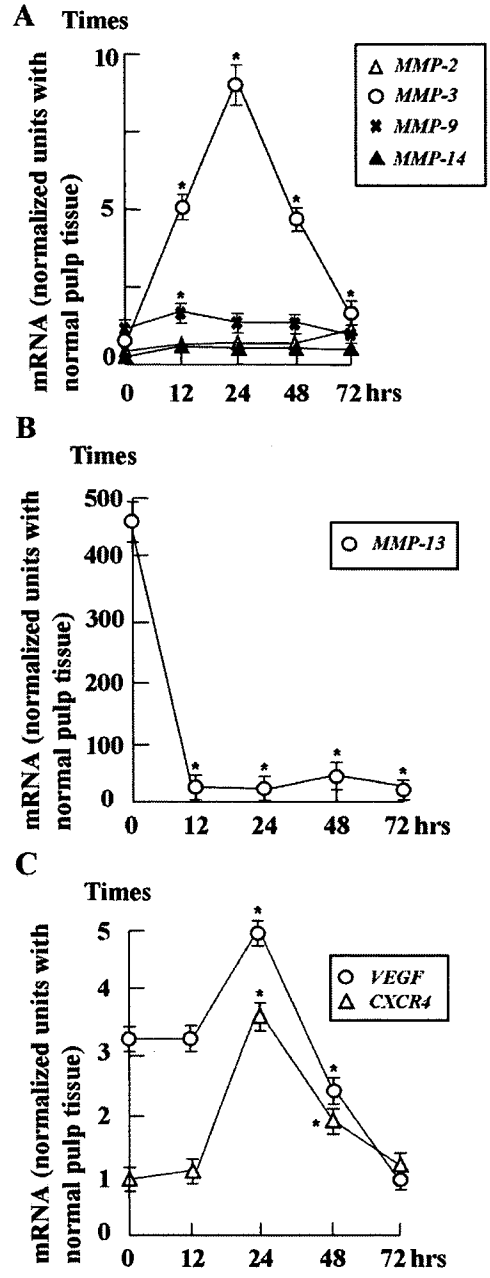

Figure 2. Real-time RT-PCR analysis of expression of mRNAs during pulp wound-healing process. **A:** Expression of MMP-2, MMP-3, MMP-9, MMP-13, and MMP-14 during pulp wound-healing process. MMP-3 showed a ninefold peak at 24 hours after injury and decreased to twofold at 72 hours. MMP-9 showed twofold expression at 12 hours. MMP-2 and MMP-14 didn't show any expression change during the healing process. **B:** MMP-13 showed 470-fold expression at immediately after injury. MMP-10 was not expressed both in normal and injured pulp. **C:** Expression of VEGF and CXCR4. VEGF showed 3.5-fold expression immediately after injury, then increased to fivefold at 24 hour after injury. CXCR4 showed 3.5-fold expression at 24 hours after injury. The experiments were repeated three times, and one representative experiment is presented (*$P < 0.05$; compared with 0 hour).

Statistical Evaluation

All data were expressed as means ± SD at four determinations. *P* values were calculated by using the unpaired Student's *t*-test. Differences were considered to be statistically significant at the $P < 0.05$ level.

Results

Histology of Pulp Tissues during Wound-Healing Process

Pulp normal and wound-healing models were constructed using rat upper incisors (Figure 1, A–D). One hour after injury, red blood cells and dilatation of blood vessels were observed. Acute inflammatory cells, such as neutrophils, infiltrated in the pulp tissue under the amputated site (Figure 1, E and F). Twenty-four hours after injury, the inflammatory cells disappeared, and a large number of fibroblast-like cells and polygonal shaped cells and new blood vessels were found in the pulp tissue under the amputated site (Figure 1, G and H). Seventy-two hours later, spindle-shaped cells were surrounded by immature collagenous matrix to form osteodentin in the upper pulp tissue under the amputated site (Figure 1, 1 and J). Seven days after injury, one to two layers of well-arranged odontoblast-like cells were found to form tubular dentin under the osteodentin (Figure 1, K and L). Pulp injury completely healed with optimal angiogenesis (Figure 1K) and accompanied by osteodentin/tubular dentin formation. Thus, these results suggested that this pulp injury model was useful for analyzing expression and function of MMPs during pulp wound-healing process.

RNA Expression during Wound-Healing Process

Expression of MMP-2, -3, -9, -10, -13, -14, VEGF, and CXCR4 mRNA was analyzed with real-time RT-PCR at 0, 12, 24, 48, and 72 hours after injury. As shown in Figure 2A, *MMP-3* was expressed nearly ninefold at 24 hours compared with control normal pulp tissue, then decreased to fourfold at 48 hours and twofold at 72 hours. MMP-9 expression showed twofold compared with control at 12 hours and decreased to the same level as 0 hour at 72 hours. MMP-13 expression was 470-fold at 0 hour, immediately after injury compared with control normal pulp, and rapidly decreased at 12 hours (Figure 2B). In contrast, expression of MMP-2 and MMP-14/MT1-MMP was continuously at the same level as control normal pulp during the pulp wound-healing process (Figure 2A). MMP-10 mRNA was not detected both in rat normal pulp and the injured pulp.

On the other hand, VEGF showed 3.5-fold expression at 0 and 12 hours after injury, then increased to 5-fold at 24 hours after injury and decreased to basal expression level at 72 hours. CXCR4 showed 3.5-fold increase in expression at 24 hours after injury (Figure 2C).

Localization of MMP-3 and CXCR4 during Pulp-Healing Process

Immediately after injury, neither MMP-3 nor CXCR4 was found in pulp (data not shown). Twenty-four hours after injury (Figure 3J), MMP-3 protein was detected in endothelial cells and/or endothelial progenitor cells in newly formed microvessels and larger vessels under the amputated site (Figure 3, A, D, and K), which positively stained with BS1-lectin (Figure 3, B and C). MMP-3 mRNA was also strongly expressed in vascular region (Figure 3M).

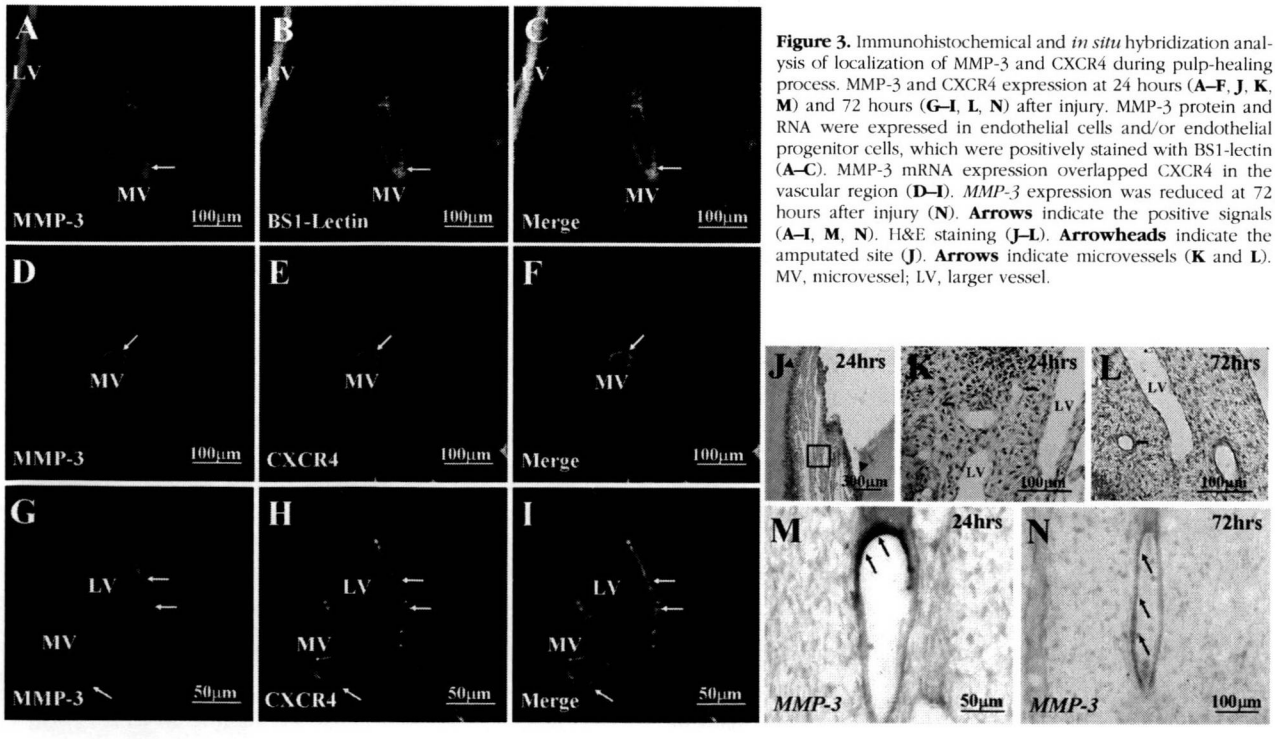

Figure 3. Immunohistochemical and *in situ* hybridization analysis of localization of MMP-3 and CXCR4 during pulp-healing process. MMP-3 and CXCR4 expression at 24 hours (**A–F, J, K, M**) and 72 hours (**G–I, L, N**) after injury. MMP-3 protein and RNA were expressed in endothelial cells and/or endothelial progenitor cells, which were positively stained with BS1-lectin (**A–C**). MMP-3 mRNA expression overlapped CXCR4 in the vascular region (**D–I**). *MMP-3* expression was reduced at 72 hours after injury (**N**). **Arrows** indicate the positive signals (**A–I, M, N**). H&E staining (**J–L**). **Arrowheads** indicate the amputated site (**J**). **Arrows** indicate microvessels (**K** and **L**). MV, microvessel; LV, larger vessel.

Double-staining immunohistochemistry showed that MMP-3 expression overlapped CXCR4 in vascular region (Figure 3, D–F). Seventy-two hours after injury (Figure 3L), MMP-3 expression also overlapped CXCR4 in microvascular and larger vessel (Figure 3, G–I). MMP-3 mRNA expression was weakly detected in vascular region (Figure 3N).

MMP-3 Stimulates Proliferation and Migration and Inhibits Apoptosis of HUVECs in Vitro

We next examined whether MMP-3 could induce the proliferation, migration, and survival (antiapoptosis) of HUVECs. As shown in Figure 4A, MMP-3 significantly increased proliferation activity of HUVECs compared with control similarly to the positive control VEGF. The proliferative effect of MMP-3 was significantly blocked by NNGH, a specific MMP-3 inhibitor. HUVECs cultured with NNGH showed a significantly reduced proliferation.

MMP-3 significantly stimulated migration activity of HUVECs in a dose-dependent manner. This effect was two times stronger compared with VEGF as a positive control and significantly blocked by NNGH (Figure 4B).

We also analyzed whether MMP-3 could inhibit the apoptosis of HUVECs. The cells cultured with 100 nmol/L/ml staurosporine for 4 hours caused apoptosis in 52% HUVECs. When cells were treated with staurosporine and MMP-3 coincidently, only 20% of cells showed apoptosis, indicating reduced apoptosis. This reduced apoptosis was completely blocked with NNGH. HUVECs cultured with staurosporine and VEGF also showed reduced apoptosis (Figure 4C).

However, MMP-10/stromelysin-2, which is a structural homologue of MMP-3, did not have any effect on proliferation, migration, and survival (antiapoptosis) of HUVECs as MMP-3 (Figure 4, A–C).

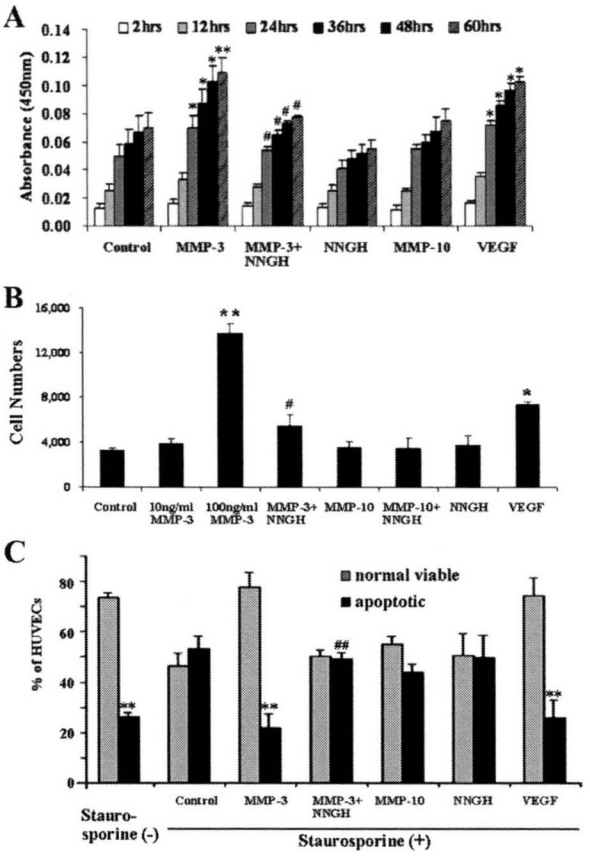

Figure 4. Effect of MMP-3 on proliferation, migration, and survival in cultured HUVECs. **A:** Enhanced proliferation by MMP-3 and VEGF. HUVECs seeded with 1000 cells per 96-well were cultured in the presence of human MMP-3 (50 ng/ml) with or without NNGH (0.13 μmol/L), MMP-10 (50 ng/ml), or VEGF-A (50 ng/ml). Cell numbers were measured by adding Tetra-color one. NNGH significantly blocked the effect of MMP-3. **B:** Induced migration by MMP-3 in a dose-dependent manner. Modified Boyden chamber assays were performed for 24 hours with polyethylene terepthlate membrane in a 24-well plate. HUVECs (10,000/well) were cultured in the upper chamber in the presence of 10 or 100 ng/ml MMP-3 with or without 0.13 μmol/L NNGH, 50 ng/ml MMP-10 with or without 0.13 μmol/L NNGH, NNGH only, or 50 ng/ml VEGF-A. The induced effect by MMP-3 was blocked by NNGH. **C:** Reduced apoptosis by MMP-3. HUVECs grown in endothelial growth medium-2 for 3 days were incubated with 100 nmol/L staurosporine in endothelial basal medium-2 supplemented with 50 ng/ml MMP-3 with or without 0.13 μmol/L NNGH, NNGH only, 50 ng/ml MMP-10, or VEGF-A. After 6 hours, the cell suspensions stained with Annexin V-FITC and propidium iodide were analyzed by flow cytometry. The cells cultured with 100 nmol/L staurosporine for 4 hours caused apoptosis in 52% of the cells. When treated together with MMP-3, only 20% of the cells showed apoptosis, indicating reduced effect on apoptosis. This effect was blocked by NNGH. Note no effect by MMP-10, a structural homologue of MMP-3. Data were expressed as means ± SD at four determinations ($^{*}P < 0.05$; $^{**}P < 0.01$, compared with the control group; $^{\#}P < 0.05$, compared with the MMP-3 group). Statistical analyses were performed by the nonpaired Student's *t*-test. The experiments were repeated three times, and one represented experiments is presented. $^{\#\#}P < 0.01$, compared with the MMP-3 group.

MMP-3 Induces Angiogenesis and Reparative Dentin Formation during Pulp Wound Healing

Next, we investigated whether MMP-3 induces angiogenesis in injured pulp *in vivo* (Figure 5A; Supplemental Figures S1–S3, see *http://ajp.amjpathol.org*). The rat incisor pulp was treated with MMP-3 in the presence or absence of NNGH. PBS was used as a negative control. Twenty-four hours after treatment, BS1-lectin-stained sections showed that the MMP-3-treated pulp exhibited more newly formed vessels compared with PBS control (Figure 5, B and C). Quantitative analysis indicated 2.0-fold increase in blood vessels in MMP-3-treated pulp compared with PBS control in the upper pulp tissue under the amputated site (Figure 5D). The presence of PCNA, a marker of cell proliferation, was examined in the sections of pulp at 24 hours after treatment. The PCNA-positive staining cells were observed significantly more—a 2.7-fold increase in number in the MMP-3-treated pulp (98.5 ± 17.7 cells/mm^2) compared with PBS control (36.0 ± 14.1 cells/mm^2) under the amputated site (Figure 5, E, F, and Q). Seventy-two hours after treatment, a large amount of reparative dentin formation was observed in the MMP-3-treated pulp compared with the PBS control (Figure 5, G–J). Intense blue-stained collagen by Masson trichrome was observed around newly differentiated odontoblasts/osteodentinoblasts in the MMP-3-treated pulp (Figure 5K). *In situ* hybridization analysis in the series sections showed that *DSPP* mRNA was expressed in the newly differentiated odontoblasts/osteodentinoblasts confined in osteodentin matrix (Figure 5L). There is no obvious odontoblasts/osteodentinoblasts in the pulp that was treated with MMP-3 in the presence of NNGH (Figure

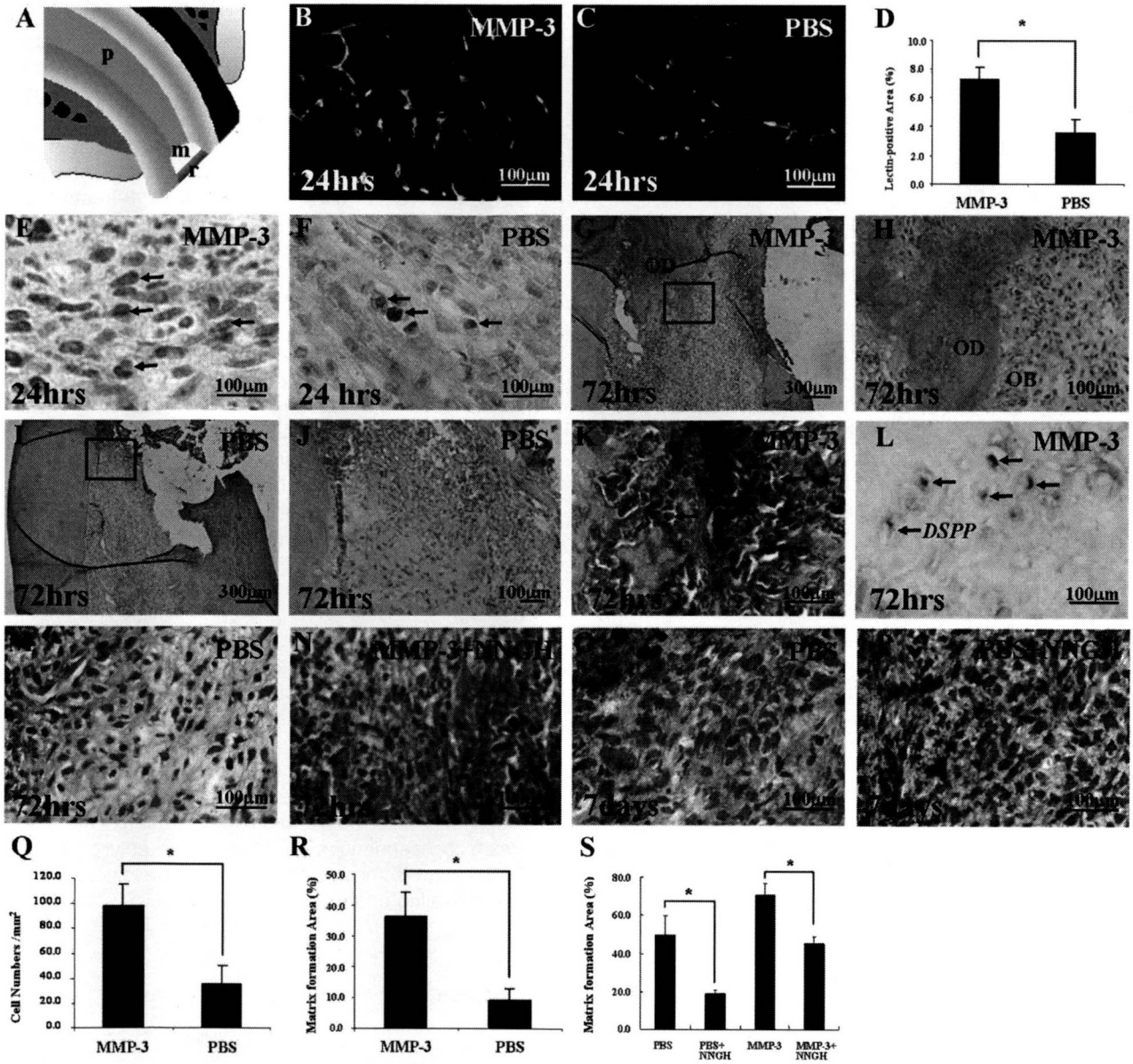

Figure 5. Acceleration of angiogenesis and pulp wound healing by MMP-3. Schematic diagrams of MMP-3 protein application on amputated pulp of rat upper incisor. **A:** The pulp cavity was filled with MMP-3 protein absorbed in spongel and resin filling. p, amputated pulp tissue; m, MMP-3 protein; r, resin (Supplemental Figures S1–S3, see *http://ajp.amjpathol.org*). Twenty-four hours after treatment (**B–F** and **Q**). Seventy-two hours after treatment (**G–N** and **R**). Seven days after treatment (**O**, **P**, **S**). BS-1-lectin staining (**B** and **C**), PCNA immunohistochemistry (**E** and **F**), H&E staining (**G–J**), Dentin sialophosphoprotein *in situ* hybridization (**L**), and Masson's trichrome staining (**K** and **M–P**) were used. **B**: Newly formed vessels in the upper part of pulp tissue under the amputated site in MMP-3-treated pulp. **C:** A few newly formed vessels in PBS control pulp. **E:** Many PCNA-positive staining cells were detected in MMP-3-treated pulp. **F:** A few PCNA-positive staining cells in PBS control pulp. **G**, magnified in **H:** A large amount of osteodentin formed under the amputated site. **I**, magnified in **J:** No osteodentin formation. **K:** Intense blue-stained collagen around newly formed osteodentinoblasts (**arrows**). **L:** Dentin sialophosphoprotein mRNA was detected in newly formed osteodentinoblasts (**arrows**). **M:** No intense blue-stained collagen and no osteodentinoblasts in PBS control. **N:** NNGH, a specific MMP-3 inhibitor, blocked the MMP-3-induced effect on osteodentin formation. **O** and **P:** Blue-stained collagen was broader in PBS control compared with that in NNGH-treated pulp on day 7. MMP-3-treated pulp (**B**, **G**, **H**, **K**) consisted of more newly formed vessels and more osteodentin compared with PBS control group (**C**, **I**, **J**, **M**). Quantitative analysis indicated that a twofold increase of blood vessels was induced by MMP-3 in the upper part of pulp tissue under the amputated site (**D**). Quantitative analysis of the PCNA-positive staining cells and collagenous matrix formation at 24 hours, 72 hours, and 7 days after treatment (**Q**, **R**, **S**). $^{*}P < 0.01$.

5N), as well as in the PBS control pulp (Figure 5, 1, J, and M) at 72 hours after treatment. The dentin matrix formation was observed significantly more—a 3.8-fold increase in area in the MMP-3-treated pulp compared with PBS control under the amputated site (Figure 5R) at 72 hours. Seven days after treatment, NNGH, a MMP-3-specific inhibitor, inhibited the dentin matrix formation significantly more compared with PBS control (Figure 5, O, P, and S).

Discussion

This is the first study to systemically detect the MMPs expressed during pulp wound-healing process and to assess the role of MMPs in injured pulp tissue. Pulp amputation is a commonly performed operation, and it leaves a clean wound, and this is a good representative acute wound model to study the profiles of biological

factors, MMPs. Rat incisor is continuously erupting tooth, and the pulp tissue has a high potential to heal after pulp injury. Rat incisor has also advantages to get many homogenous samples of injured pulp tissue at once, and not take so much time before complete healing compared with canine teeth. Therefore, we have used the rat pulp injury model[27] to examine expression of MMPs during pulp wound healing process.

We have recently isolated pulp-derived $CD31^-$; $CD146^-$ side population cells having a highly vasculogenic potential. MMP-3 was highly expressed in $CD31^-$; $CD146^-$ side population cells compared with $CD31^+$; $CD146^-$ side population cells without vasculogenic potential as well as total pulp cells.[28] Both MMP-9 and MMP-2 were very weakly expressed in those cell fractions.[28] When $CD31^-$;$CD146^-$ side population cells were transplanted on the amputated pulp in dogs, the transplanted cells were migrating in the vicinity of the newly formed vasculature and expressed proangiogenic factors, including MMP-3, implying trophic actions on endothelial cells (K. Iohara et al, unpublished data). A previous report has shown that MMPs are induced immediately following injury and show reproducible expression patterns.[29] In the present study, MMP-3 significantly increased at 24 hours after pulp injury, and MMP-9 weakly increased at 12 hours. MMP-13 was highly increased immediately after injury and rapidly decreased at 12 hours. MMP-2 and MMP-14 were not found to be changed. Therefore, we have focused our further study on MMP-3 to assess the role of MMPs in angiogenesis and pulp wound healing.

In the present study, MMP-3 was localized in endothelial cells and/or endothelial progenitor cells. MMP-3-positive cells expressed CXCR4, a marker of endothelial cells.[30] MMP-3 enhanced proliferation and migration activities and had an antiapoptotic effect on endothelial cells *in vitro*. The similar stimulatory effects of MMP-3 on cell proliferation and migration have also been reported in a human glioblastoma cell line after enhanced gene expression of MMP-3 by platelet-derived growth factor receptor-α.[31] The high expression of MMP-3 is also reported in the endometrial regenerative cells, a novel stem cell population from the endometrium, which is involved in the angiogenesis phase of the menstrual cycle.[32] Furthermore, topical MMP-3 protein application on the injured pulp significantly enhanced angiogenesis and proliferation under the amputated pulp at 24 hours after treatment. Therefore, these results suggest that MMP-3 induces proliferation, migration, and survival of endothelial cells, leading to angiogenesis. On the other hand, angiogenic factors, such as VEGF, basic fibroblast growth factor, and transforming growth factor-β, can be released from extracellular matrix/basement membrane by MMPs degradation,[33] suggesting that MMP-3 also regulates angiogenesis in an indirect way.

Protein application of growth/differentiation factors such as transforming growth factor-β1, insulin-like growth factor-I and bone morphogentic proteins has been demonstrated to promote reparative dentin formation on the injured/amputated pulp because of their inductive effect on odontoblast differentiation.[16] However, there had been no report thus far on reparative dentin formation by an endopeptidase catalyzing the turnover and degradation of ECM protein. In the present study, MMP-3 had no stimulatory effect on differentiation of pulp stem/progenitor cells into odontoblasts *in vitro* (data not shown), although it enhanced activity of proliferation, migration, and survival of endothelial cells. Angiogenesis and reparative dentin formation were accelerated in MMP-3-treated pulp compared with PBS control in the rat pulp injury model. Therefore, induced reparative dentin formation might be indirect effect of MMP-3. However, the liberation and modification of the variety of growth/differentiation factors and cytokines embedded in dentin matrix and/or extracellular substrate by MMP-3 might cause some inductive effects on differentiation of pulp stem/progenitor cells into odontoblasts and reparative dentin formation *in vivo*.[6] MMPs, including MMP-3, are associated with re-epithelialization, which is the regrowth of epithelia over a denuded surface.[34] Wound healing is delayed in MMP-3 null mice, suggesting MMP-3 also contributes to wound healing.[35] MMP-1 protein application in mouse muscle injury increases myofibril formation and myogenic regeneration through either the digestion of scar tissues or activation of muscle cell migration.[36] However, there has been no report on direct topical application of MMP-3 protein in any disease and any injury thus far. Our present results of stimulatory effect on angiogenesis and acceleration of wound-healing events by MMP-3 in the pulp injury might be a useful clue for future clinical treatment for dental pulp. Developing rational therapy for dentin/pulp regeneration requires further identification of specific MMP-3 substrates and characterization of the downstream consequences of MMP-3 proteolytic activity. MMP-3 may also have a more general role in accelerating wound healing or improving angiogenesis.

References

1. Rundhaug JE: Matrix metalloproteinases and angiogenesis. J Cell Mol Med 2005, 9:267–285
2. Massova I, Kotra LP, Fridman R, Mobashery S: Matrix metalloproteinases: structures, evolution, and diversification. FASEB J 1998, 12:1075–1095
3. Nagase H, Woessner JF, Jr.: Matrix metalloproteinases. J Biol Chem 1999, 274:21491–21494
4. Chang C, Werb Z: The many faces of metalloproteases: cell growth, invasion, angiogenesis and metastasis. Trends Cell Biol 2001, 11:S37–S43
5. Chakraborti S, Mandal M, Das S, Mandal A, Chakraborti T: Regulation of matrix metalloproteinases: an overview. Mol Cell Biochem 2003, 253:269–285
6. Ra HJ, Parks WC: Control of matrix metalloproteinase catalytic activity. Matrix Biol 2007, 26:587–596
7. Sternlicht MD, Werb Z: How matrix metalloproteinases regulate cell behavior. Annu Rev Cell Dev Biol 2001, 17:463–516
8. Kahari VM, Saarialho-Kere U: Matrix metalloproteinases and their inhibitors in tumour growth and invasion. Ann Med 1999, 31:34–45
9. Ravanti L, Kahari VM: Matrix metalloproteinases in wound repair (review). Int J Mol Med 2000, 6:391–407
10. Vu TH, Werb Z: Matrix metalloproteinases: effectors of development and normal physiology. Genes Dev 2000, 14:2123–2133
11. Mott JD, Werb Z: Regulation of matrix biology by matrix metalloproteinases. Curr Opin Cell Biol 2004, 16:558–564
12. Grunewald M, Avraham I, Dor Y, Bachar-Lustig E, Itin A, Jung S, Chimenti S, Landsman L, Abramovitch R, Keshet E: VEGF-induced

adult neovascularization: recruitment, retention, and role of accessory cells. Cell 2006, 124:175–189
13. Hsu JY, McKeon R, Goussev S, Werb Z, Lee JU, Trivedi A, Noble-Haeusslein LJ: Matrix metalloproteinase-2 facilitates wound healing events that promote functional recovery after spinal cord injury. J Neurosci 2006, 26:9841–9850
14. Kadirvel R, Dai D, Ding YH, Danielson MA, Lewis DA, Cloft HJ, Kallmes DF: Endovascular treatment of aneurysms: healing mechanisms in a Swine model are associated with increased expression of matrix metalloproteinases, vascular cell adhesion molecule-1, and vascular endothelial growth factor, and decreased expression of tissue inhibitors of matrix metalloproteinases. AJNR Am J Neuroradiol 2007, 28:849–856
15. Shima I, Katsuda S, Ueda Y, Takahashi N, Sasaki H: Expression of matrix metalloproteinases in wound healing after glaucoma filtration surgery in rabbits. Ophthalmic Res 2007, 39:315–324
16. Nakashima M, Akamine A: The application of tissue engineering to regeneration of pulp and dentin in endodontics. J Endod 2005, 31:711–718
17. Yamamura T: Differentiation of pulpal cells and inductive influences of various matrices with reference to pulpal wound healing. J Dent Res 1985, 64 Spec No:530–540
18. Roberts-Clark DJ, Smith AJ: Angiogenic growth factors in human dentine matrix. Arch Oral Biol 2000, 45:1013–1016
19. Mathieu S, El-Battari A, Dejou J, About I: Role of injured endothelial cells in the recruitment of human pulp cells. Arch Oral Biol 2005, 50:109–113
20. Tran-Hung L, Mathieu S, About I: Role of human pulp fibroblasts in angiogenesis. J Dent Res 2006, 85:819–823
21. Stokowski A, Shi S, Sun T, Bartold PM, Koblar SA, Gronthos S: EphB/ephrin-B interaction mediates adult stem cell attachment, spreading, and migration: implications for dental tissue repair. Stem Cells 2007, 25:156–164
22. Gusman H, Santana RB, Zehnder M: Matrix metalloproteinase levels and gelatinolytic activity in clinically healthy and inflamed human dental pulps. Eur J Oral Sci 2002, 110:353–357
23. Tsai CH, Chen YJ, Huang FM, Su YF, Chang YC: The up-regulation of matrix metalloproteinase-9 in inflamed human dental pulps. J Endod 2005, 31:860–862
24. Zhou B, Ma FX, Liu PX, Fang ZH, Wang SL, Han ZB, Poon MC, Han ZC: Impaired therapeutic vasculogenesis by transplantation of OxLDL-treated endothelial progenitor cells. J Lipid Res 2007, 48:518–527
25. Zheng L, Yamashiro T, Fukunaga T, Balam TA, Takano-Yamamoto T: Bone morphogenetic protein 3 expression pattern in rat condylar cartilage, femoral cartilage and mandibular fracture callus. Eur J Oral Sci 2005, 113:318–325
26. Strakova Z, Szmidt M, Srisuparp S, Fazleabas AT: Inhibition of matrix metalloproteinases prevents the synthesis of insulin-like growth factor binding protein-1 during decidualization in the baboon. Endocrinology 2003, 144:5339–5346
27. Imai M, Hayashi Y: Ultrastructure of wound healing following direct pulp capping with calcium-β-glycerophosphate (Ca-BGP). J Oral Pathol Med 1993, 22:411–417
28. Iohara K, Zheng L, Wake H, Ito M, Nabekura J, Wakita H, Nakamura H, Into T, Matsusita K, Nakashima M: A novel stem cell source for vasculogenesis in ischemia: subfraction of side population cells from dental pulp. Stem Cells 2008, 26:2408–2418
29. Le NT, Xue M, Castelnoble LA, Jackson CJ: The dual personalities of matrix metalloproteinases in inflammation. Front Biosci 2007, 12:1475–1487
30. Volin MV, Joseph L, Shockley MS, Davies PF: Chemokine receptor CXCR4 expression in endothelium. Biochem Biophys Res Commun 1998, 242:46–53
31. Laurent M, Martinerie C, Thibout H, Hoffman MP, Verrecchia F, Le Bouc Y, Mauviel A, Kleinman HK: NOVH increases MMP-3 expression and cell migration in glioblastoma cells via a PDGFR-α-dependent mechanism. FASEB J 2003, 17:1919–1921
32. Meng X, Ichim TE, Zhong J, Rogers A, Yin Z, Jackson J, Wang H, Ge W, Bogin V, Chan KW, Thebaud B, Riordan NH: Endometrial regenerative cells: a novel stem cell population. J Transl Med 2007, 5:57
33. Raffetto JD, Khalil RA: Matrix metalloproteinases and their inhibitors in vascular remodeling and vascular disease. Biochem Pharmacol 2008, 75:346–359
34. Gill SE, Parks WC: Metalloproteinases and their inhibitors: regulators of wound healing. Int J Biochem Cell Biol 2008, 40:1334–1347
35. Bullard KM, Lund L, Mudgett JS, Mellin TN, Hunt TK, Murphy B, Ronan J, Werb Z, Banda MJ: Impaired wound contraction in stromelysin-1-deficient mice. Ann Surg 1999, 230:260–265
36. Bedair H, Liu TT, Kaar JL, Badlani S, Russell AJ, Li Y, Huard J: Matrix metalloproteinase-1 therapy improves muscle healing. J Appl Physiol 2007, 102:2338–2345

Molecular Immunology 46 (2009) 2080–2089

Contents lists available at ScienceDirect

Molecular Immunology

journal homepage: www.elsevier.com/locate/molimm

IL-4 alters expression patterns of storage components of vascular endothelial cell-specific granules through STAT6- and SOCS-1-dependent mechanisms

Megumi Inomata[a,b], Takeshi Into[c,*], Misako Nakashima[b], Toshihide Noguchi[a], Kenji Matsushita[b,*]

[a] Department of Periodontology, School of Dentistry, Aichigakuin University, Nagoya 464-8650, Japan
[b] Department of Oral Disease Research, National Institute for Longevity Sciences, National Center for Geriatrics and Gerontology, Obu, Aichi 474-8522, Japan
[c] Department of Oral Microbiology, Asahi University School of Dentistry, Mizuho, Gifu 501-0296, Japan

ARTICLE INFO

Article history:
Received 9 January 2009
Received in revised form 10 February 2009
Accepted 14 February 2009
Available online 5 May 2009

Keywords:
Weibel–Palade body
IL-4
STAT6
SOCS-1
Vascular endothelial cell

ABSTRACT

IL-4 develops Th2-biased immunity or allergic inflammation through activation of STAT6-dependent signaling. In vascular endothelial cells (ECs), IL-4 elicits regulatory effects on chemokine production and adhesion molecule expression to recruit T cells and eosinophils. In this study, we examined how IL-4 affects Weibel–Palade bodies (WPBs), EC-specific storage granules capable to store multiple protein components, including von Willebrand factor (vWF), P-selectin, eotaxin-3, IL-8 and angiopoietin-2 (Ang-2). Among 11 WPB component genes that we examined, IL-4 potently upregulated the expression levels of P-selectin and eotaxin-3, whereas it downregulated the expression levels of IL-8 and Ang-2. Both regulatory effects were dependent on STAT6. In addition, the IL-4-induced downregulatory effect on WPB component genes depended on the negative feedback regulation by SOCS-1 induced by STAT6 signaling. Furthermore, IL-4-regulated gene expression through STAT6 and SOCS-1 was consistent with WPB compositional changes in cultivated ECs and capillary-like tube networks. Since WPBs enable ECs to rapidly regulate multiple critical functions of vasculatures, IL-4-induced alteration of expression patterns of WPB storage components may convert the physiological functions of WPBs into Th2-biased immune functions or allergic functions.

1. Introduction

The pleiotropic cytokine IL-4 is produced by Th2 cells, eosinophils, basophils and mast cells and is associated with immune protection against helminthic parasites. Dysregulation of IL-4 expression often leads to the development of allergic reactions and chronic inflammatory diseases (Lee and Hirani, 2006; Li-Weber and Krammer, 2003; Tepper et al., 1990; Wills-Karp, 1999). IL-4 exerts its activities via binding to cell surface IL-4 receptor complexes, IL-4Rα with the common γ chain (type I IL-4 receptor) or with IL-13Rα1 (type II IL-4 receptor) (Chatila, 2004; Nelms et al., 1999). IL-4 ligation triggers activation of tyrosine kinases JAK1 and JAK3, which phosphorylate tyrosine residues in the cytoplasmic domain of IL-4Rα and common γ chain, respectively. This event then activates signal transducer and activator of transcription 6 (STAT6), resulting in its homodimerization and subsequent translocation into the nucleus, where it regulates gene transcription (Chatila, 2004; Takeda et al., 1996). So far, more than 35 different STAT6 target genes have been identified, and it has been shown that many of them are involved in Th2-associated immune processes (Hebenstreit et al., 2006).

In vascular endothelial cells (ECs), IL-4 regulates expression of adhesion molecules, with an upregulatory effect on VCAM-1 and a downregulatory effect on E-selectin, and regulates production of CC chemokines, including MCP-1 and eotaxins (Lampinen et al., 2004; Lukacs, 2001; Øynebråten et al., 2004; Schleimer et al., 1992; Shinkai et al., 1999; Yao et al., 1996). This shift in the balance of expression of adhesion molecules and chemokine production by IL-4 is thought to favor the recruitment of T cells and eosinophils, rather than neutrophils and basophils, from the bloodstream to the surface of the endothelium, leading to their infiltration into a site of allergic inflammation (Schleimer et al., 1992; Shinkai et al., 1999; Thornhill et al., 1990). In addition, IL-4-induced selective recruitment of such cells is partly mediated by STAT6-dependent expression of P-selectin/CD62P and eotaxin-3/CCL26 in ECs (Lampinen et al., 2004). However, it is not fully understood how IL-4 alters normal functions of ECs into Th2-biased or allergic functions.

Abbreviations: Ang-2, angiopoietin-2; EC, endothelial cell; LAMP-3, lysosomal-associated membrane protein 3; OPG, osteoprotegerin; qRT-PCR, quantitative real-time reverse transcription-polymerase chain reaction; SOCS, suppressor of cytokine signaling; STAT6, signal transducer and activator of transcription 6; t-PA, tissue plasminogen activator; vWF, von Willebrand factor; WPB, Weibel–Palade body.

* Corresponding authors. Tel.: +81 58 329 1422; fax: +81 58 329 1422.
E-mail addresses: into@dent.asahi-u.ac.jp (T. Into), kmatsu30@nils.go.jp (K. Matsushita).

0161-5890/$ – see front matter © 2009 Elsevier Ltd. All rights reserved.
doi:10.1016/j.molimm.2009.02.015

ECs have specific storage granules, designated Weibel–Palade bodies (WPBs) (Weibel and Palade, 1964). WPBs were originally identified as an intracellular storage vehicle for von Willebrand factor (vWF), a plasma protein that mediates platelet adhesion, but an increasing number of other components, including P-selectin, eotaxin-3, IL-8/CXCL8, angiopoietin-2 (Ang-2), lysosomal-associated membrane protein 3 (LAMP-3)/CD63, endothelin-1, tissue plasminogen activator (t-PA) and osteoprotegerin (OPG), has been revealed to be present within WPBs (Metcalf et al., 2008; Rondaij et al., 2006). The features of WPB components indicates a crucial role for degranulation of WPBs, which provides the endothelium with the ability to rapidly respond to changes in the micro-environment and to regulate multiple biological functions of vasculatures, such as inflammation, hemostasis, vascular tone regulation and angiogenesis. Regulated degranulation of WPBs can be initiated through an increase in intracellular calcium or cyclic adenosine monophosphate level following stimulation of ECs with thrombin, histamine, TNF, bacterial products or extracellular adenosine triphosphate (Inomata et al., 2007; Into et al., 2007; Metcalf et al., 2008; Rondaij et al., 2006).

Several studies have demonstrated that inflammatory cytokines, such as TNF-α and IL-1β, induce proinflammatory IL-8 production in ECs, enabling storage of IL-8 within WPBs as "memory" of past EC reactions (Utgaard et al., 1998; Wolff et al., 1998). Such a change in WPB components may lead to alteration of normal physiological features of WPBs into proinflammatory features. We therefore hypothesized that IL-4 alters the normal expression pattern of WPB components into patterns associated with Th2-biased immunity or allergic diseases. In this study, we first examined whether IL-4 alters expression levels of WPB component genes in ECs. We here report that IL-4 regulates expression levels of several WPB component genes through a STAT6-dependent mechanism. We also examined whether such changes in gene expression are indeed consistent with WPB compositional changes.

2. Materials and methods

2.1. Reagents, plasmids and cell culture

Human rIL-4 was obtained from R&D Systems. Histamine was obtained from Sigma–Aldrich. An expression plasmid encoding myc-SOCS-1 was a kind gift from Akihiko Yoshimura (Division of Molecular and Cellular Immunology, Medical Institute of Bioregulation, Kyushu University). Human umbilical vein endothelial cells (HUVECs) were purchased from Cambrex (at least 3 different lots isolated from different donors), grown in EBM-2 complete endothelial growth medium (Cambrex) under 5% CO_2 at 37 °C and used for experiments from passages 4 to 8. HUVECs were stimulated with IL-4 after reaching confluence. IL-4 did not influence cell survival and proliferation in the confluent HUVEC culture (data not shown).

2.2. Gene expression analysis by quantitative real-time reverse transcription-polymerase chain reaction

Total RNA was prepared from HUVECs using an RNeasy extraction kit (Qiagen). One μg of total RNA was reverse-transcribed using ReverTraAce reverse transcriptase (TOYOBO) with both an oligo21dT primer and a random 6 primer set. qRT-PCR was performed using Power SYBR Green PCR Master Mix (Applied Biosystems) on a 7300 Fast Real-Time PCR System (Applied Biosystems) according to the manufacturer's instructions. All primer sequences are listed in Supporting Table 1. We confirmed that there was no critical difference between the values normalized to the levels of three different house-keeping genes, *Gapdh*, *Ppia1* and *Hprt1*. Results shown in this study were normalized to the level of *Gapdh*.

2.3. DNA transfection and RNA interference

DNA transfection in HUVECs was performed using Opti-MEM I (Invitrogen) and Lipofectin reagent (Invitrogen) as described previously (Into et al., 2007). 'ON-TARGET *plus*' siRNAs for human *Stat6* (006690) and *Socs1* (011511) and a non-targeting control RNA (D-001810-01) were purchased from Dharmacon. siRNA sequences were provided by the manufacturer. Transfection of siRNA in HUVECs was performed as described previously (Inomata et al., 2007). After 24 h of incubation, the transfection media were changed and cells were used for experiments.

2.4. Capillary-like tube formation

For formation of capillary-like tube networks in vitro, HUVECs were harvested and resuspended in 200 μl EBM-2 and then seeded at a density of 1×10^5 cells in 24-well plates onto the surface of 150 μl of polymerized Matrigel (Becton Dickinson). After 12 h of incubation at 37 °C, Matrigel containing EC tubes was pervaded with EBM-2 containing 10 ng/ml IL-4 and then incubated for an additional 48 h. IL-4 did not affect the number of capillary-like tubules when experiments were performed after tubule formation (data not shown). To fix the tubes in gels, incubation media were carefully removed and 1 ml of methanol was added to the culture, followed by incubation at room temperature for 30 min.

2.5. Immunofluorescent staining of WPBs

Immunofluorescent staining of WPBs was performed by reference to our protocols described previously (Into et al., 2008; Into et al., 2007). Briefly, HUVECs were fixed at −20 °C with methanol for 30 min. Then cells or capillary-like cells in Matrigel were treated with an anti-vWF rabbit polyclonal antibody (sc-14014, Santa Cruz Biotechnology) and an anti-P-selectin mouse monoclonal antibody (sc-19672, Santa Cruz Biotechnology) at room temperature for 1 h. The former primary antibody was detected with Alexa Fluor 488-conjugated anti-mouse IgG antibody (Invitrogen) and the latter antibody was detected with Alexa Fluor 568-conjugated anti-rabbit IgG antibody (Invitrogen). To avoid background staining of Matrigel by antibodies, potassium chloride at a final concentration of 200 mM was added to the antibody solution while staining. The detection of Ang-2 was performed using an anti-Ang-2 goat polyclonal antibody (AF623, R&D Systems) and Alexa Fluor 568-conjugated anti-goat IgG antibody (Invitrogen). Images were obtained by a fluorescent microscope IX71 with DP70 image capture (Olympus) in the presence of Prolong Gold antifade reagent (Invitrogen) and then processed using Adobe Photoshop, version 7.0.

2.6. Immunoblotting

Confluent HUVEC seeded on 60 mm plates were stimulated or unstimulated with IL-4 for 48 h. The cytoplasmic cell lysates were obtained by incubating cells with a buffer consisting of 20 mM Tris–hydrochloride (pH 7.2), 150 mM sodium chloride, 5 mM EDTA and 1% Triton X-100 and protease inhibitor cocktails (Roche) at 4 °C for 15 min, followed by clarification by centrifugation at 12,000 × *g* for 10 min. These cell lysates were diluted by an equal volume of SDS sample buffer consisting of 0.5 M Tris–hydrochloride (pH 7.2), 10% glycerol, 2% SDS, 5% 2-mercaptoethanol and 0.05% bromphenol blue. Samples were boiled for 5 min and separated under reducing conditions on 12% SDS–PAGE gels and then transferred onto polyvinylidene fluoride membranes. Membranes were blocked at room temperature for 1 h with 5% non-fat skim milk solved in PBS and then reacted with primary antibodies to IL-8 (sc-7922), eotaxin-3 (sc-19353), Ang-2 (sc-20718) and GAPDH (sc-25778) (all

from Santa Cruz Biotechnology) for 1 h. Immunoreactive bands were visualized by an ECL system (Amersham Pharmacia Biotech) after being treated with HRP-conjugated secondary antibodies to anti-mouse and anti-rabbit IgG.

2.7. Statistics

All values were evaluated by statistical analysis using one-way ANOVA and Student–Newman–Keul's test. Differences were considered to be statistically significant at the level of $p < 0.05$.

3. Results

3.1. IL-4 regulates expression patterns of WPB component genes

WPBs are vWF-containing condensing vesicles, the formation of which involves several steps of vWF protein processing, including intramolecular disulfide bonding, maturation by the propeptide portion within the molecule, and multimerisation (Metcalf et al., 2008; Rondaij et al., 2006). WPBs have the capability to store multiple protein components, but these components are required to be abundantly expressed with vWF to be processed and recruited to WPBs at the trans-Golgi network. Utilizing qRT-PCR, we first examined the effect of IL-4 on gene expression levels of 11 WPB components in HUVECs. IL-4 decreased mRNA expression of vWF (*Vwf*), but the effect was very modest during stimulation for 48 h (Fig. 1). Consistent with previous results for human ECs (Shinkai et al., 1999; Stein et al., 2008; Yao et al., 1996), IL-4 greatly increased mRNA expression levels of P-selectin (*Selp*) and eotaxin-3 (*Ccl26*) and slightly increased the levels of OPG (*Tnfrsf11b*) and fucosyltransferase 4 (*Fut4*) (Fig. 1). In contrast, IL-4 gradually decreased mRNA expression levels of IL-8 (*Il8*), Ang-2 (*Angpt2*) and LAMP-3/CD63 (*Lamp3*). Also, the levels of endothelin-1 (*Edn1*), endothelin-converting enzyme 1 (*Ece1*) and t-PA (*Plat*) were slightly deceased (Fig. 1). Thus, IL-4 has the capability to both positively and negatively regulate expression levels of WPB component genes.

3.2. IL-4-regulated proteins are stored in WPBs

We next examined whether such changes in gene expression levels are indeed consistent with WPB compositional changes. One of the best understood and most important storage components of WPBs is P-selectin, a type I transmembrane adherent protein expressed in platelets and ECs (Hannah et al., 2002; Johnston et al., 1989; McEver et al., 1989). Immunofluorescent staining of HUVECs revealed the presence of a considerable amount of vWF-positive granules, indicative of WPBs, but a considerably low level of P-selectin expression (Fig. 2A, left). After IL-4 stimulation, a considerable amount of P-selectin was produced in more than 60% of cells (Fig. 2A, middle) and was stored partly within WPBs (Fig. 2A, middle and right). Remarkable changes in vWF expression or numbers of WPBs were not observed in the cells. These vWF- and P-selectin-positive granules completely disappeared from the cells after stimulation with histamine (Supporting Fig. 1), indicating that P-selectin was stored and released as a WPB component. P-selectin was not stored within specific organisms in several cells lacking vWF-positive granules but was diffusedly present in the cell membrane (Fig. 2A, middle).

ECs on culture plates show a cobblestone-like morphology, whereas ECs cultured in extracellular matrix gels undergo formation of capillary-like tube networks. We investigated whether IL-4-induced P-selectin storage in WPBs also occurs in ECs forming tube networks. vWF-positive WPBs were observed in tube-forming HUVECs (Fig. 2B). We found that P-selectin-positive WPBs were increased in cells stimulated with IL-4 (Fig. 2B).

We next investigated Ang-2 expression in WPBs, since *Angpt2* expression was decreased after IL-4 stimulation as shown in Fig. 1.

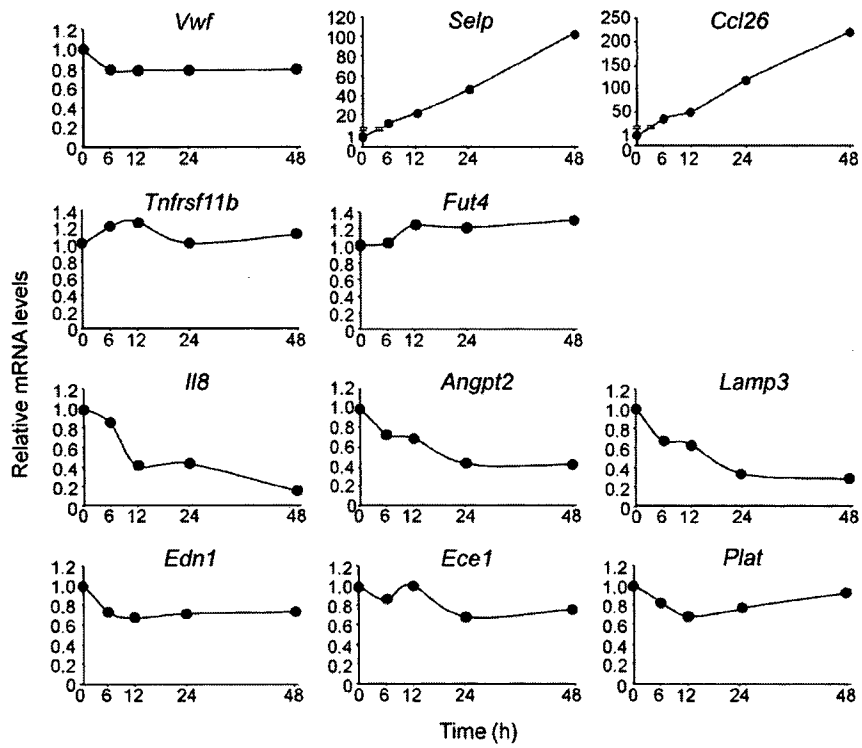

Fig. 1. IL-4 modulates gene expression patterns of WPB components. HUVECs were stimulated with 10 ng/ml IL-4 for the indicated periods. Then the mRNA expression levels of WPB component genes were determined by qRT-PCR. Each value is normalized to the mRNA level of GAPDH. Results were calculated as 'fold increase' when the control cells were taken as 1 and are expressed as means ± SD of three independent determinations.

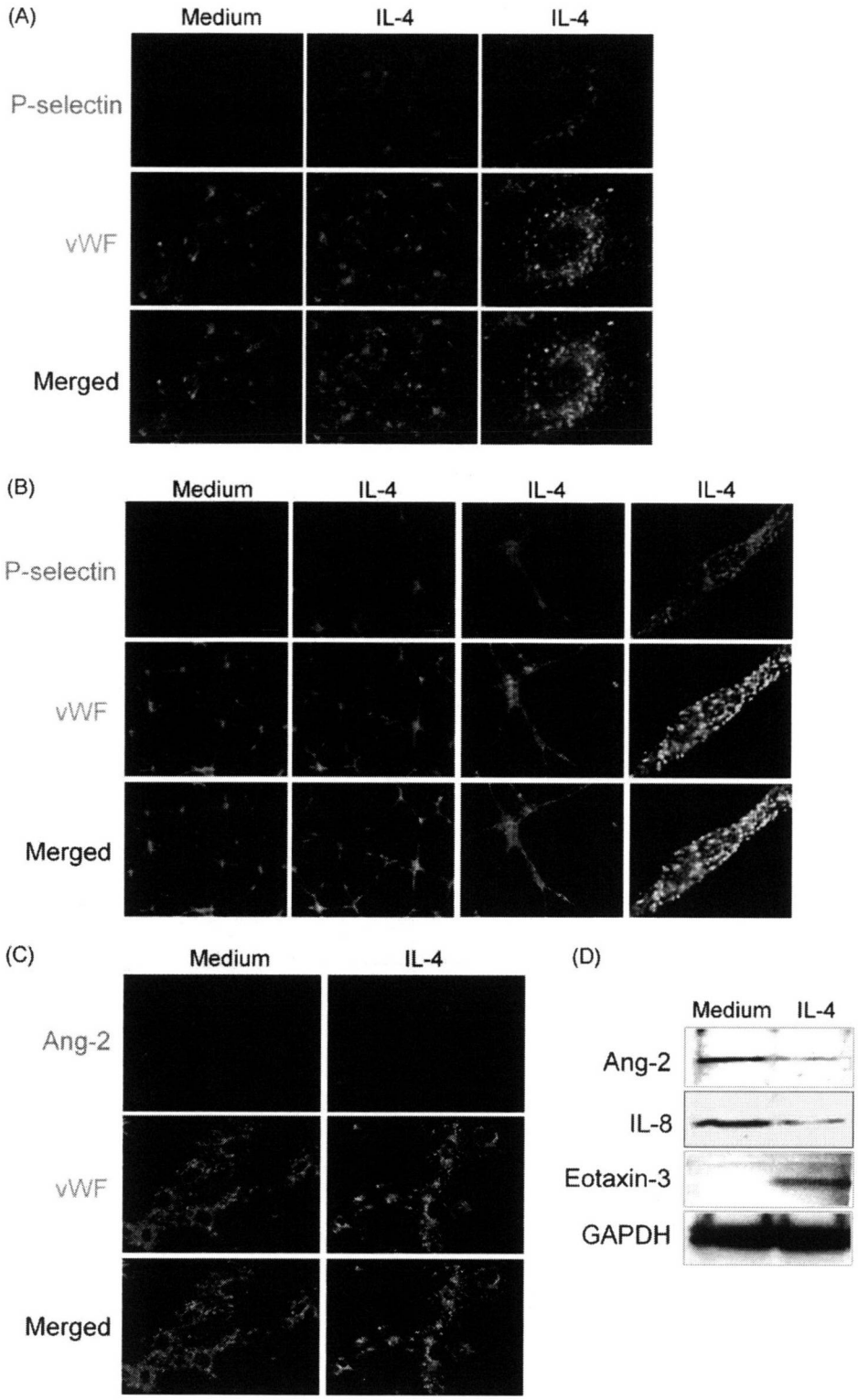

Fig. 2. IL-4-induced P-selectin protein is stored in WPBs. (A) HUVECs that had been cultured with or without 10 ng/ml IL-4 for 48 h were fixed and stained immunofluorescently with antibodies to P-selectin (red) and vWF (green). Scale bar: 50 μm. (B) Capillary-like tube networks were formed by culturing HUVECs in Matrigel. Tubes were cultured with or without 10 ng/ml IL-4 for 48 h. The cells were then fixed and stained immunofluorescently with antibodies to P-selectin (red) and vWF (green) in the presence of 200 mM potassium chloride. Scale bar: 50 μm. (C) HUVECs stimulated with or not stimulated with 10 ng/ml IL-4 for 48 h were fixed and stained immunofluorescently with antibodies to Ang-2 (red) and vWF (green). All results are representative of three independent experiments. (D) HUVECs stimulated with or not stimulated with 10 ng/ml IL-4 for 48 h were lysed for immunoblot analysis for the intracellular expression of Ang-2, IL-8, eotaxin-3 and GAPDH. Results are representative of two independent experiments. (For interpretation of the references to color in this figure legend, the reader is referred to the web version of the article.)

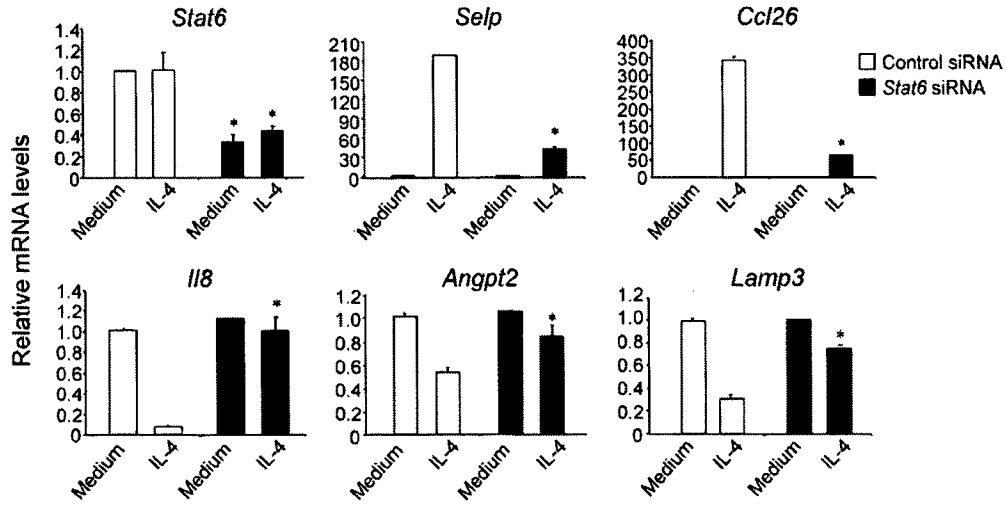

Fig. 3. STAT6 mediates IL-4-induced alteration of the expression levels of WPB component genes. HUVECs transfected with STAT6-specific or control siRNA were cultured with or without 10 ng/ml IL-4 for 48 h. The mRNA expression levels of STAT6, P-selectin, eotaxin-3, IL-8, Ang-2 and LAMP-3 were determined by qRT-PCR. Each value is normalized to the mRNA level of GAPDH and is expressed as the mean ± SD ($n = 3$). *, *versus* cells transfected with control siRNA, $P < 0.05$.

Immunofluorescent staining revealed that Ang-2 was stored in vWF-positive WPBs (Fig. 2C). Although IL-4 stimulation slightly decreased Ang-2 expression, the effect was very modest, as was found for vWF and number of WPBs. Thus, by this method, it was difficult to clearly detect decreased WPB components stored in WPBs at least within 48 h of stimulation. To detect intracellular Ang-2 protein more clearly, we performed immunoblotting for the cytoplasmic lysates obtained from HUVECs. As the result, IL-4 obviously decreased the intracellular expression level of Ang-2 (Fig. 2D). Furthermore, IL-4 also decreased the basal intracellular expression level of IL-8. In contrast to Ang-2 and IL-8, IL-4 increased expression level of eotaxin-3 (Fig. 2D). These results suggest that decreased gene expression levels of WPB components are also correlated with WPB storage.

3.3. *STAT6 mediates IL-4-induced alteration of expression levels of WPB component genes*

STAT6, the critical signaling molecule in the IL-4R pathway, is known to serve as a positive and negative regulator of IL-4-induced gene expression (Hebenstreit et al., 2006). To assess the involvement of STAT6 in IL-4 regulation of expression levels of WPB component genes, we utilized *Stat6*-specific siRNA. Expression of STAT6 mRNA (*Stat6*) was observed in HUVECs and was not altered by IL-4 stimulation (Fig. 3). Effective *Stat6* reduction was confirmed in cells transfected with *Stat6* siRNA (Fig. 3). IL-4-induced expression of P-selectin and eotaxin-3 mRNAs was remarkably decreased by *Stat6* knockdown (Fig. 3). Furthermore, IL-4-induced decrease in mRNA expression of Ang-2, IL-8 and LAMP-3 was restored by *Stat6*

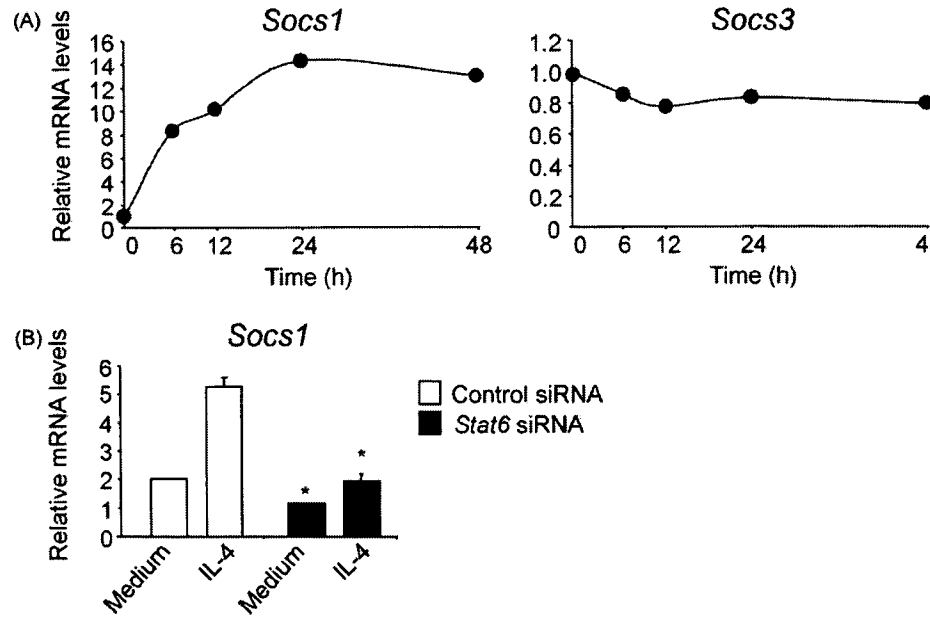

Fig. 4. SOCS-1 is induced by IL-4 in ECs. (A) HUVECs were stimulated with 10 ng/ml IL-4 for the indicated periods. The mRNA expression levels of SOCS-1 and SOCS-3 were determined by qRT-PCR. Results were calculated as 'fold increase' when the control cells were taken as 1 and are expressed as means ± SD of three independent determinations. (B) HUVECs transfected with STAT6-specific or control siRNA were cultured with or without 10 ng/ml IL-4 for 48 h. The mRNA expression level of SOCS-1 was determined by quantitative qRT-PCR. Each value is normalized to the mRNA level of GAPDH and is expressed as the mean ± SD ($n = 3$). *, *versus* cells transfected with control siRNA, $P < 0.05$.

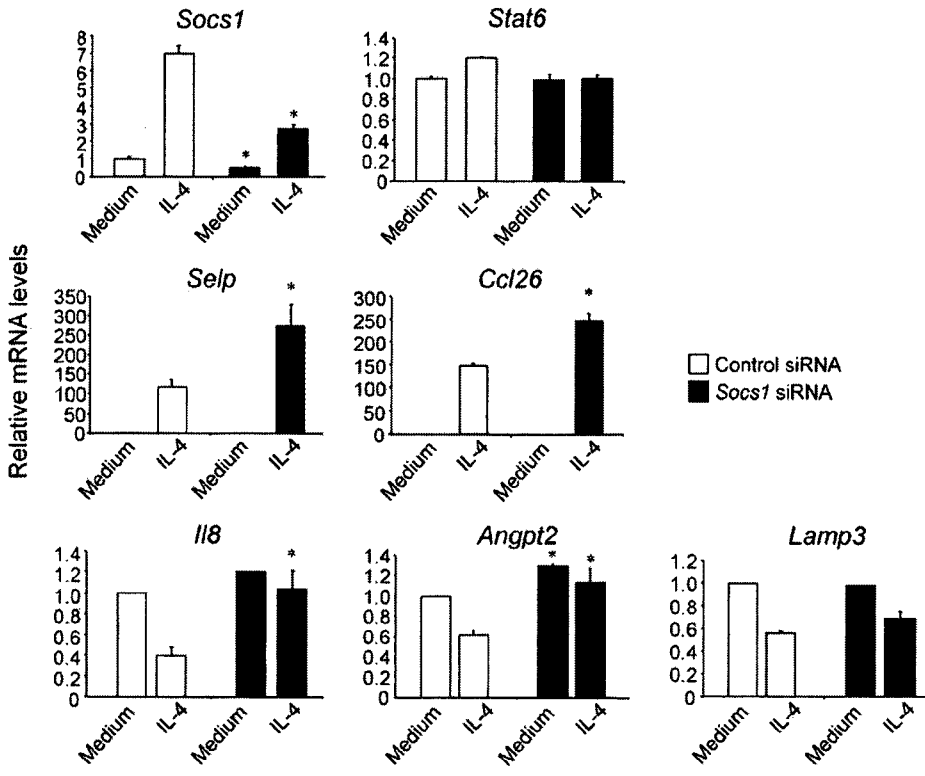

Fig. 5. Endogenous SOCS-1 is a regulator of IL-4-induced alteration of the expression levels of WPB component genes. HUVECs transfected with SOCS-1-specific or control siRNA were cultured with or without 10 ng/ml IL-4 for 48 h. The mRNA expression levels of SOCS-1, STAT6, P-selectin, eotaxin-3, IL-8, Ang-2 and LAMP-3 were determined by qRT-PCR. Each value is normalized to the mRNA level of GAPDH and is expressed as the mean ± SD ($n = 3$). *, *versus* cells transfected with control siRNA, $P < 0.05$.

knockdown (Fig. 3). Thus, not only upregulatory but also downregulatory effects of IL-4 on expression levels of WPB component genes are dependent on STAT6.

3.4. SOCS-1 mediates IL-4-induced alteration of expression levels of WPB component genes

It is known that SOCS-1 and SOCS-3, members of inducible feedback inhibitors of cytokine signaling pathways, are potent inhibitors of the IL-4R-STAT6 pathway (Yoshimura et al., 2007). In HUVECs, IL-4 could induce SOCS-1, but not SOCS-3, after IL-4 stimulation (Fig. 4A). Consistent with previous results in other cell types (Hebenstreit et al., 2003; Losman et al., 1999), IL-4-induced *Socs1* expression was dependent on STAT6 (Fig. 4B). To assess the involvement of SOCS-1 in IL-4 regulation of expression levels of WPB component genes, we utilized *Socs1*-specific siRNA. We confirmed that IL-4-induced SOCS-1 expression was efficiently reduced in HUVECs transfected with *Socs1* siRNA (Fig. 5). Expression of STAT6 mRNA was not altered by knockdown of *Socs1*. IL-4-induced mRNA expression of P-selectin and eotaxin-3 was considerably enhanced by knockdown of *Socs1* (Fig. 5). In addition, the downregulatory effect of IL-4 on mRNA expression of IL-8 and Ang-2 was clearly attenuated by knockdown of *Socs1* (Fig. 5). The expression level of LAMP-3 mRNA was not restored by knockdown of *Socs1*, indicating that LAMP-3 downregulation is mediated by another mechanism.

To confirm the effects of SOCS-1 on IL-4 regulation of gene expression, we utilized a DNA construct encoding c-Myc epitope-tagged SOCS-1 (myc-SOCS-1), the expression of which could be discriminated from that of endogenous *Socs1* in HUVECs (Fig. 6A). Expression of P-selectin and eotaxin-3 was significantly attenuated by myc-SOCS-1 expression (Fig. 6B). In contrast, myc-SOCS-1 enhanced the downregulatory effect of IL-4 on expression levels of IL-8 and Ang-2 mRNAs, but not LAMP-3 mRNA (Fig. 6B). Thus, these results clearly indicate that IL-4 increases SOCS-1 expression through STAT6 and then downregulates IL-8 and Ang-2 via negative feedback regulation.

3.5. STAT6 and SOCS-1 are regulators of IL-4-induced P-selectin storage in WPBs

Experiments were then carried out to determine whether STAT6 and SOCS-1 regulated IL-4-induced P-selectin storage within WPBs. P-selectin-positive granules were not observed in IL-4-stimulated HUVECs transfected with STAT6 siRNA (Fig. 7A). Similarly, P-selectin-positive granules were not observed in IL-4-stimulated HUVECs expressing myc-SOCS-1 (Fig. 7A). *Stat6* siRNA and myc-SOCS-1 did not alter vWF expression and the number of WPBs (Fig. 7A). Similar results were obtained in HUVECs forming capillary-like tubes (Fig. 7B). These results indicate that STAT6 and SOCS-1 are important mediators of IL-4-induced storage component changes in WPBs.

4. Discussion

Our study demonstrated that IL-4 affects expression patterns of WPB component genes through STAT6- and SOCS-1-dependent mechanisms. IL-4 could induce WPB compositional change after alteration of gene expression, at least of the upregulated components P-selectin (Fig. 2) and eotaxin-3 (Øynebråten et al., 2004). Although we could not demonstrate apparent changes in IL-4-downregulated components within WPBs by immunofluorescent staining, immunoblot analyses revealed that IL-4 stimulation clearly decreased the expression of such components within intracellular compartments (Fig. 2D). Given that WPBs enable ECs to rapidly regulate multiple critical functions of vasculatures, IL-4-

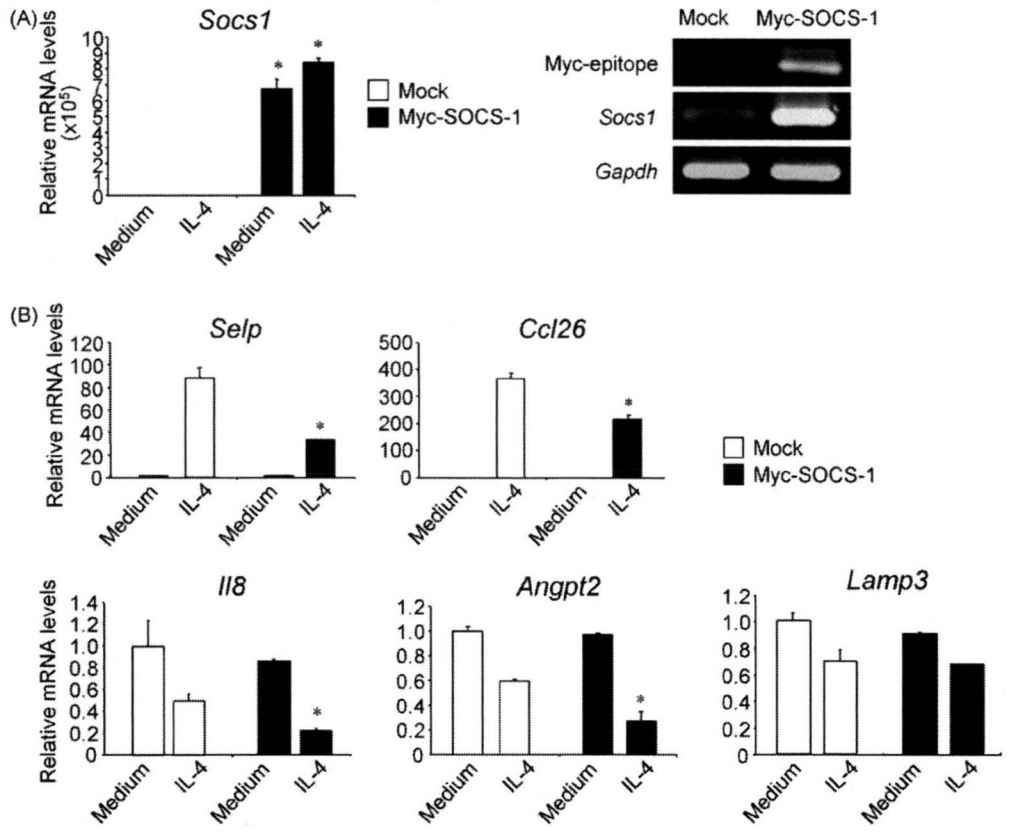

Fig. 6. Exogenous SOCS-1 regulates IL-4-induced alteration of the expression levels of WPB component genes. (A) HUVECs transfected with a plasmid encoding myc-SOCS-1 or a control plasmid (mock) were cultured with or without 10 ng/ml IL-4 for 48 h. The mRNA expression levels of SOCS-1 were determined by qRT-PCR. Each value is normalized to the mRNA level of GAPDH and is expressed as the mean ± SD ($n = 3$). Expression levels of myc-SOCS-1, total SOCS-1 (endogenous SOCS-1 and myc-SOCS-1) and GAPDH were also analyzed by agarose gel electrophoresis (right picture). *, *versus* cells transfected with a control plasmid, $P < 0.05$. (B) HUVECs transfected with a plasmid encoding myc-SOCS-1 or a control plasmid (mock) were cultured with or without 10 ng/ml IL-4 for 48 h. The mRNA expression levels of P-selectin, eotaxin-3, IL-8, Ang-2 and LAMP-3 were determined by qRT-PCR. Each value is normalized to the mRNA level of GAPDH and is expressed as the mean ± SD ($n = 3$). *, *versus* cells transfected with a control plasmid, $P < 0.05$.

induced alteration of the expression pattern of WPB components may convert the physiological functions of WPBs into the functions for Th2-biased immunity or allergic inflammation through STAT6 and SOCS-1.

STAT6 has been thought to be essential for IL-4- and IL-13-mediated immune functions. It is currently known that IL-4-induced cell differentiation is largely dependent on STAT6, whereas IL-4 can regulate cell proliferation and survival at least partially through STAT6-independent mechanisms, such as via PI3K and MAPKs (Hebenstreit et al., 2006; Jiang et al., 2000). Indeed, IL-4 regulates many gene expression levels through STAT6-dependent and STAT6-independent mechanisms (Chen et al., 2003; Levings and Schrader, 1999). Our results showed that both positive and negative regulatory effects of IL-4 on expression of several WPB component genes were completely dependent on STAT6 (Fig. 3). Such effects of STAT6 are consistent with results of previous studies showing that STAT6 serves as a positive and negative regulator of IL-4-induced gene expression in T and B lymphocytes (Chen et al., 2003; Schroder et al., 2002). These effects are thought to be mediated partly through STAT6-dependent induction of several transcriptional factors and SOCSs (Chen et al., 2003; Canfield et al., 2005; Losman et al., 1999). Since STAT6-deficient mice exhibit impaired immune responses to infection with nematodes and allergic responses in murine models of asthma because of impaired differentiation of T and B lymphocytes (Akimoto et al., 1998; Takeda et al., 1996), future studies must focus on how STAT6-dependent WPB component regulation affects such immune or allergic reactions.

The SOCS family is comprised of eight members, each of which contains an SH2 domain and a conserved C-terminal module termed the SOCS box (Yoshimura et al., 2007). Most SOCS proteins are induced by cytokines and therefore act in a negative feedback loop to inhibit cytokine signal transduction. It has been reported that IL-4 induces expression of two SOCSs, SOCS-1 through a STAT-6-dependent mechanism and SOCS-3 through a STAT6-independent but p38 MAPK-dependent mechanism (Canfield et al., 2005). In ECs, however, IL-4 could only induce expression of SOCS-1 through STAT6 (Fig. 4). We therefore focused on SOCS-1 in this study, although the IL-4R-STAT6 pathway has been reported to be negatively regulated by both SOCS-1 and SOCS-3 (Hebenstreit et al., 2005). SOCS-1 is known to inhibit the STAT6 pathway through direct interaction with JAK via a kinase inhibitory region and to promote its degradation in proteasome via an activity like E3 ubiquitin ligase (Yoshimura et al., 2007). Indeed, we showed that SOCS-1 elicited a negative regulatory effect on IL-4-induced expression of P-selectin and eotaxin-3 (Fig. 5). We also found that IL-4 downregulatory effects on IL-8 and Ang-2 were mediated by SOCS-1 (Fig. 5), indicating that STAT6-dependent downregulatory effects are negative feedback regulation by SOCS-1. SOCS-1 did not affect the expression of STAT6 (Fig. 5). Although the reason for the downregulatory effects by SOCS-1 is not completely clear, several lines of evidence obtained in previous studies may partly provide an explanation. For example, SOCS-1 has the ability to directly interact with the p65 subunit of NF-κB and enhance its ubiquitinylation and degradation (Ryo et al., 2003), which may lead to downregulation of the expression of NF-κB-driven genes, including IL-8 and E-selectin. Further

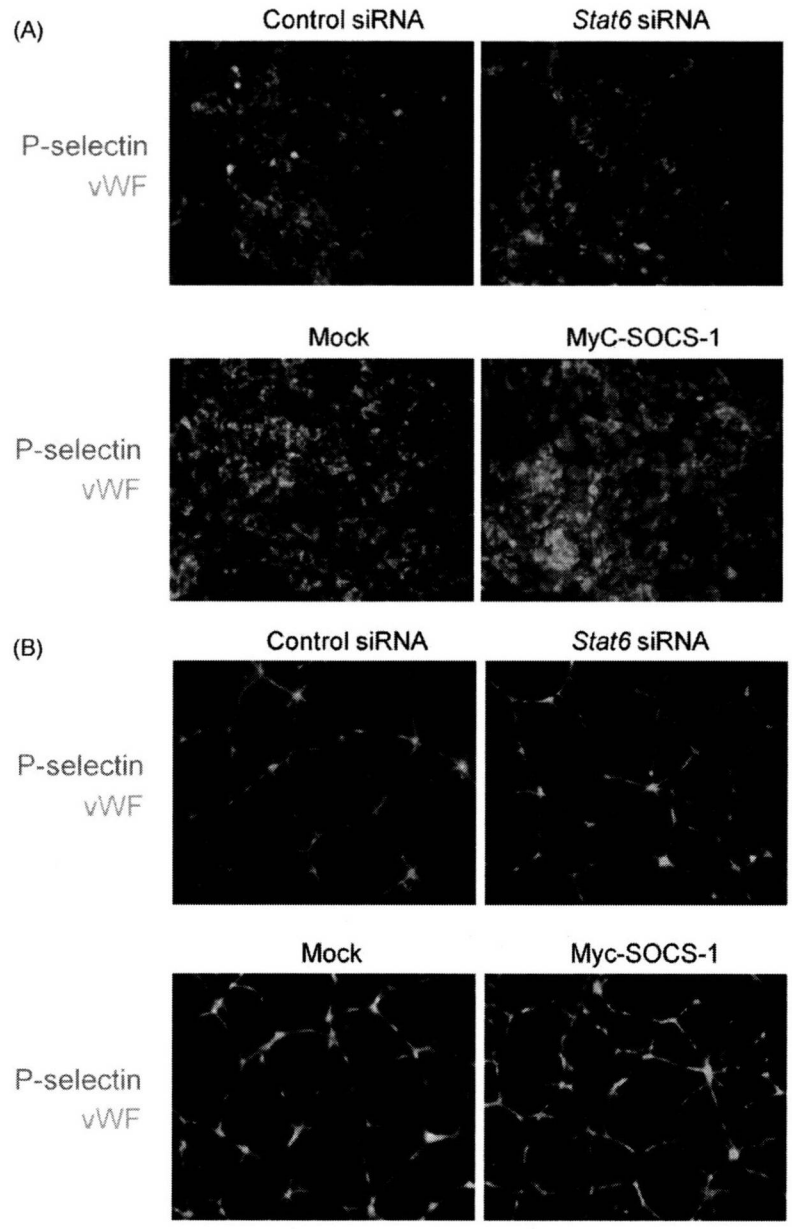

Fig. 7. STAT6 and SOCS-1 regulate IL-4-induced P-selectin protein storage in WPBs. (A) HUVECs were transfected with STAT6-specific or control siRNA or with a plasmid encoding myc-SOCS-1 or a control plasmid (mock). Cells were stimulated with 10 ng/ml IL-4 for 48 h and then fixed and stained immunofluorescently with antibodies to P-selectin (red) and vWF (green). Results are representative of three independent experiments. (B) HUVECs were transfected with STAT6-specific or control siRNA or with a plasmid encoding myc-SOCS-1 or a control plasmid (mock). Capillary-like tube networks were formed by culturing these HUVECs in Matrigel. Cells were stimulated with 10 ng/ml IL-4 for 48 h and then fixed and stained immunofluorescently with antibodies to P-selectin (red) and vWF (green). Results are representative of three independent experiments. (For interpretation of the references to color in this figure legend, the reader is referred to the web version of the article.)

research is needed to determine in detail the effects of STAT6 and SOCS-1 on IL-4 regulation of WPB components and EC functions.

Condensed storage pools of multiple components within WPBs are a preliminary arrangement of ECs for a rapid release of them in response to acute extracellular stimuli to regulate multiple functions in vasculatures (Rondaij et al., 2006). The importance of component localization within WPBs has been shown by studies using vWF knockout mice, lacking the formation of WPBs in ECs (Denis et al., 2001). These animals show inflammatory defects, similar to those seen in P-selectin knockouts, partially because of mislocation of P-selectin and defects of its transportation to the cell membrane. P-selectin, eotaxin-3 and IL-8 are known to be directly involved in rapid recruitment of bloodstream leukocytes to the endothelium. Ang-2 regulates destabilization of quiescent endothelia and then sensitization of them towards angiogenic factors and proinflammatory cytokines (Fiedler et al., 2006). Although the function of LAMP-3 in ECs has been unclear, it is known that a blocking Ab to LAMP-3 inhibits neutrophil adhesion to ECs stimulated with thrombin (Toothill et al., 1990). We demonstrated that IL-4 potently promoted the expression of P-selectin and eotaxin-3 and decreased the expression of IL-8, Ang-2 and LAMP-3 (Fig. 1). Therefore, upon secondary stimulation, such as stimulation by mast cell-derived histamine, of IL-4-primed ECs, profuse amounts of P-selectin and eotaxin-3 may be released from WPBs to the luminal surface of ECs. Such reactions may provide a rapid pathway for Th2-biased responses of ECs, such as specific recruitment of eosinophils to sites of allergic and chronic inflammation. Although IL-4 can attenuate angiogenesis (Nishimura et al., 2008; Volpert et al., 1998), the role

of the EC reactions in dysregulation of angiogenesis, which is often seen in allergic or chronic inflammatory diseases (Puxeddu et al., 2005), is currently unknown.

5. Conclusions

IL-4 plays a role in immune protection against helminthic parasites and pathogenesis of allergic inflammation through promoting IgE production, Th2 cell differentiation and Th2 cytokine-mediated immune activation through activation of STAT6 signaling. Although the importance of WPBs in Th2-biased or allergic functions of ECs has not been clear, our current study revealed the possibility that IL-4 also has a priming role in regulation of EC functions through WPB compositional changes through STAT6- and SOCS-1-dependent mechanisms. Studies in progress will further elucidate its role and importance in mediating the biological effects of WPBs in the immune regulation and development of allergic or chronic inflammation.

Acknowledgements

This work was supported by Grants-in-Aid for Scientific Research on Priority Areas (19041079 to T.I.), for Scientific Research (B: 19390538 to K.M.) and for Exploratory Research (19659494 to K.M.), provided by the Ministry of Education, Culture, Sports, Science and Technology, Japan. We heartily thank Akihiko Yoshimura (Division of Molecular and Cellular Immunology, Medical Institute of Bioregulation, Kyushu University) for providing us with a DNA construct of SOCS-1.

Appendix A. Supplementary data

Supplementary data associated with this article can be found, in the online version, at doi:10.1016/j.molimm.2009.02.015.

References

Akimoto, T., Numata, F., Tamura, M., Takata, Y., Higashida, N., Takashi, T., Takeda, K., Akira, S., 1998. Abrogation of bronchial eosinophilic inflammation and airway hyperreactivity in signal transducers and activators of transcription (STAT)6-deficient mice. J. Exp. Med. 187, 1537–1542.

Canfield, S., Lee, Y., Schroder, A., Rothman, P., 2005. Cutting edge: IL-4 induces suppressor of cytokine signaling-3 expression in B cells by a mechanism dependent on activation of p38 MAPK. J. Immunol. 174, 2494–2498.

Chatila, T.A., 2004. Interleukin-4 receptor signaling pathways in asthma pathogenesis. Trends Mol. Med. 10, 493–499.

Chen, Z., Lund, R., Aittokallio, T., Kosonen, M., Nevalainen, O., Lahesmaa, R., 2003. Identification of novel IL-4/Stat6-regulated genes in T lymphocytes. J. Immunol. 171, 3627–3635.

Denis, C.V., Andre, P., Saffaripour, S., Wagner, D.D., 2001. Defect in regulated secretion of P-selectin affects leukocyte recruitment in von Willebrand factor-deficient mice. Proc. Natl. Acad. Sci. U.S.A. 98, 4072–4077.

Fiedler, U., Reiss, Y., Scharpfenecker, M., Grunow, V., Koidl, S., Thurston, G., Gale, N.W., Witzenrath, M., Rosseau, S., Suttorp, N., Sobke, A., Herrmann, M., Preissner, K.T., Vajkoczy, P., Augustin, H.G., 2006. Angiopoietin-2 sensitizes endothelial cells to TNF-α and has a crucial role in the induction of inflammation. Nat. Med. 12, 235–239.

Hannah, M.J., Williams, R., Kaur, J., Hewlett, L.J., Cutler, D.F., 2002. Biogenesis of Weibel–Palade bodies. Semin. Cell. Dev. Biol. 13, 313–324.

Hebenstreit, D., Luft, P., Schmiedlechner, A., Duschl, A., Horejs-Hoeck, J., 2005. SOCS-1 and SOCS-3 inhibit IL-4 and IL-13 induced activation of Eotaxin-3/CCL26 gene expression in HEK293 cells. Mol. Immunol. 42, 295–303.

Hebenstreit, D., Luft, P., Schmiedlechner, A., Regl, G., Frischauf, A.M., Aberger, F., Duschl, A., Horejs-Hoeck, J., 2003. IL-4 and IL-13 induce SOCS-1 gene expression in A549 cells by three functional STAT6-binding motifs located upstream of the transcription initiation site. J. Immunol. 171, 5901–5907.

Hebenstreit, D., Wirnsberger, G., Horejs-Hoeck, J., Duschl, A., 2006. Signaling mechanisms, interaction partners, and target genes of STAT6. Cytokine Growth Factor Rev. 17, 173–188.

Inomata, M., Into, T., Ishihara, Y., Nakashima, M., Noguchi, T., Matsushita, K., 2007. Arginine-specific gingipain A from *Porphyromonas gingivalis* induces Weibel–Palade body exocytosis and enhanced activation of vascular endothelial cells through protease-activated receptors. Microbes Infect. 9, 1500–1506.

Into, T., Inomata, M., Nakashima, M., Shibata, K., Hacker, H., Matsushita, K., 2008. Regulation of MyD88-dependent signaling events by S nitrosylation retards Toll-like receptor signal transduction and initiation of acute-phase immune responses. Mol. Cell. Biol. 28, 1338–1347.

Into, T., Kanno, Y., Dohkan, J., Nakashima, M., Inomata, M., Shibata, K., Lowenstein, C.J., Matsushita, K., 2007. Pathogen recognition by Toll-like receptor 2 activates Weibel–Palade body exocytosis in human aortic endothelial cells. J. Biol. Chem. 282, 8134–8141.

Jiang, H., Harris, M.B., Rothman, P., 2000. IL-4/IL-13 signaling beyond JAK/STAT. J. Allergy Clin. Immunol. 105, 1063–1070.

Johnston, G.I., Cook, R.G., McEver, R.P., 1989. Cloning of GMP-140, a granule membrane protein of platelets and endothelium: sequence similarity to proteins involved in cell adhesion and inflammation. Cell 56, 1033–1044.

Lampinen, M., Carlson, M., Hakansson, L.D., Venge, P., 2004. Cytokine-regulated accumulation of eosinophils in inflammatory disease. Allergy 59, 793–805.

Lee, Y.W., Hirani, A.A., 2006. Role of interleukin-4 in atherosclerosis. Arch. Pharm. Res. 29, 1–15.

Levings, M.K., Schrader, J.W., 1999. IL-4 inhibits the production of TNF-α and IL-12 by STAT6-dependent and -independent mechanisms. J. Immunol. 162, 5224–5229.

Li-Weber, M., Krammer, P.H., 2003. Regulation of IL4 gene expression by T cells and therapeutic perspectives. Nat. Rev. Immunol. 3, 534–543.

Losman, J.A., Chen, X.P., Hilton, D., Rothman, P., 1999. Cutting edge: SOCS-1 is a potent inhibitor of IL-4 signal transduction. J. Immunol. 162, 3770–3774.

Lukacs, N.W., 2001. Role of chemokines in the pathogenesis of asthma. Nat. Rev. Immunol. 1, 108–116.

McEver, R.P., Beckstead, J.H., Moore, K.L., Marshall-Carlson, L., Bainton, D.F., 1989. GMP-140, a platelet α-granule membrane protein, is also synthesized by vascular endothelial cells and is localized in Weibel–Palade bodies. J. Clin. Invest. 84, 92–99.

Metcalf, D.J., Nightingale, T.D., Zenner, H.L., Lui-Roberts, W.W., Cutler, D.F., 2008. Formation and function of Weibel–Palade bodies. J. Cell. Sci. 121, 19–27.

Nelms, K., Keegan, A.D., Zamorano, J., Ryan, J.J., Paul, W.E., 1999. The IL-4 receptor: signaling mechanisms and biologic functions. Annu. Rev. Immunol. 17, 701–738.

Nishimura, Y., Nitto, T., Inoue, T., Node, K., 2008. IL-13 attenuates vascular tube formation via JAK2-STAT6 pathway. Circ. J. 72, 469–475.

Øynebråten, I., Bakke, O., Brandtzaeg, P., Johansen, F.E., Haraldsen, G., 2004. Rapid chemokine secretion from endothelial cells originates from 2 distinct compartments. Blood 104, 314–320.

Puxeddu, I., Ribatti, D., Crivellato, E., Levi-Schaffer, F., 2005. Mast cells and eosinophils: a novel link between inflammation and angiogenesis in allergic diseases. J. Allergy Clin. Immunol. 116, 531–536.

Rondaij, M.G., Bierings, R., Kragt, A., van Mourik, J.A., Voorberg, J., 2006. Dynamics and plasticity of Weibel–Palade bodies in endothelial cells. Arterioscler. Thromb. Vasc. Biol. 26, 1002–1007.

Ryo, A., Suizu, F., Yoshida, Y., Perrem, K., Liou, Y.C., Wulf, G., Rottapel, R., Yamaoka, S., Lu, K.P., 2003. Regulation of NF-kappaB signaling by Pin1-dependent prolyl isomerization and ubiquitin-mediated proteolysis of p65/RelA. Mol. Cell 12, 1413–1426.

Schleimer, R.P., Sterbinsky, S.A., Kaiser, J., Bickel, C.A., Klunk, D.A., Tomioka, K., Newman, W., Luscinskas, F.W., Gimbrone Jr., M.A., McIntyre, B.W., et al., 1992. IL-4 induces adherence of human eosinophils and basophils but not neutrophils to endothelium. Association with expression of VCAM-1. J. Immunol. 148, 1086–1092.

Schroder, A.J., Pavlidis, P., Arimura, A., Capece, D., Rothman, P.B., 2002. Cutting edge: STAT6 serves as a positive and negative regulator of gene expression in IL-4-stimulated B lymphocytes. J. Immunol. 168, 996–1000.

Shinkai, A., Yoshisue, H., Koike, M., Shoji, E., Nakagawa, S., Saito, A., Takeda, T., Imabeppu, S., Kato, Y., Hanai, N., Anazawa, H., Kuga, T., Nishi, T., 1999. A novel human CC chemokine, eotaxin-3, which is expressed in IL-4-stimulated vascular endothelial cells, exhibits potent activity toward eosinophils. J. Immunol. 163, 1602–1610.

Stein, N.C., Kreutzmann, C., Zimmermann, S.P., Niebergall, U., Hellmeyer, L., Goettsch, C., Schoppet, M., Hofbauer, L.C., 2008. Interleukin-4 and interleukin-13 stimulate the osteoclast inhibitor osteoprotegerin by human endothelial cells through the STAT6 pathway. J. Bone Miner. Res. 23, 750–758.

Takeda, K., Tanaka, T., Shi, W., Matsumoto, M., Minami, M., Kashiwamura, S., Nakanishi, K., Yoshida, N., Kishimoto, T., Akira, S., 1996. Essential role of Stat6 in IL-4 signalling. Nature 380, 627–630.

Tepper, R.I., Levinson, D.A., Stanger, B.Z., Campos-Torres, J., Abbas, A.K., Leder, P., 1990. IL-4 induces allergic-like inflammatory disease and alters T cell development in transgenic mice. Cell 62, 457–467.

Thornhill, M.H., Kyan-Aung, U., Haskard, D.O., 1990. IL-4 increases human endothelial cell adhesiveness for T cells but not for neutrophils. J. Immunol. 144, 3060–3065.

Toothill, V.J., Van Mourik, J.A., Niewenhuis, H.K., Metzelaar, M.J., Pearson, J.D., 1990. Characterization of the enhanced adhesion of neutrophil leukocytes to thrombin-stimulated endothelial cells. J. Immunol. 145, 283–291.

Utgaard, J.O., Jahnsen, F.L., Bakka, A., Brandtzaeg, P., Haraldsen, G., 1998. Rapid secretion of prestored interleukin 8 from Weibel–Palade bodies of microvascular endothelial cells. J. Exp. Med. 188, 1751–1756.

Volpert, O.V., Fong, T., Koch, A.E., Peterson, J.D., Waltenbaugh, C., Tepper, R.I., Bouck, N.P., 1998. Inhibition of angiogenesis by interleukin 4. J. Exp. Med. 188, 1039–1046.

Weibel, E.R., Palade, G.E., 1964. New cytoplasmic components in arterial endothelia. J. Cell. Biol. 23, 101–112.

Wills-Karp, M., 1999. Immunologic basis of antigen-induced airway hyperresponsiveness. Annu. Rev. Immunol. 17, 255–281.
Wolff, B., Burns, A.R., Middleton, J., Rot, A., 1998. Endothelial cell "memory" of inflammatory stimulation: human venular endothelial cells store interleukin 8 in Weibel–Palade bodies. J. Exp. Med. 188, 1757–1762.
Yao, L., Pan, J., Setiadi, H., Patel, K.D., McEver, R.P., 1996. Interleukin 4 or oncostatin M induces a prolonged increase in P-selectin mRNA and protein in human endothelial cells. J. Exp. Med. 184, 81–92.
Yoshimura, A., Naka, T., Kubo, M., 2007. SOCS proteins, cytokine signalling and immune regulation. Nat. Rev. Immunol. 7, 454–465.

Regeneration of dental pulp after pulpotomy by transplantation of CD31$^-$/CD146$^-$ side population cells from a canine tooth

Aim: To achieve complete regeneration of dental pulp *in vivo* by stem/progenitor cells obtained from a fraction of side population (SP) cells from canine pulp. **Materials & methods:** A subfraction of SP cells, CD31$^-$/CD146$^-$ SP cells, were isolated by flow cytometry from canine dental pulp. The efficiency of this subfraction of SP cells was evaluated in an experimental model of pulp injury in the dog. **Results:** The fractionated SP cells formed extensive networks of tube-like structures *in vitro*. Transplantation of the SP cells into an *in vivo* model of amputated pulp resulted in complete regeneration of pulp tissue with capillaries and neuronal cells within 14 days. Gene-expression studies demonstrated the expression of pro-angiogenic factors, implying trophic action on endothelial cells. **Conclusions:** This investigation demonstrates the potential utility of fractionated SP cells as a source of cells for total pulp regeneration complete with angiogenesis and vasculogenesis.

KEYWORDS: amputated pulp CD31 dental pulp stem cells dentinogenesis pulp regeneration side population cells

Koichiro Iohara, Li Zheng, Masataka Ito, Ryo Ishizaka, Hiroshi Nakamura, Takeshi Into, Kenji Matsushita & Misako Nakashima

Author for correspondence

Department of Oral Disease Research, National Institute for Longevity Sciences, National Center for Geriatrics & Gerontology, Obu, Aichi 474-8522, Japan

Tel.: +81 562 44 5651 ext. 5069; Fax: +81 562 46 8684

E-mail: misako@nils.go.jp

Department of Developmental Anatomy & Regenerative Medicine, National Defense Medical College, Tokorozawa, Saitama 359-8513, Japan

Department of Pediatric Dentistry, School of Dentistry, Aichigakuin University, Nagoya, Aichi 464-8651, Japan

Department of Endodontology, School of Dentistry, Aichigakuin University, Nagoya, Aichi 464-8651, Japan

Dental caries is one of the most prevailing health problems, causing early loss of dental pulp and resultant tooth loss. Dental pulp is critical for maintenance of homeostasis of teeth and essential for longevity of teeth and quality of life. Therefore, regeneration of pulp is an unmet need in endodontics and dentistry. The vascular system in dental pulp plays a role in nutrition and oxygen supply and functions as a conduit for the transport of metabolic waste. Cellular elements of blood vessels, such as endothelial cells, pericytes and associated cells, and nerves contribute to pulpal homeostasis. Thus, angiogenesis/vasculogenesis and neurogenesis are critical for pulp regeneration [1]. Vascularization during pulpal wound repair and regeneration may be due to angiogenesis (formation of blood vessels by endothelial cells) and vasculogenesis (formation of new blood vessels by angioblasts derived from bone marrow and by endothelial progenitor cells from circulating peripheral blood) [2]. The precise origin and mechanism of angiogenesis/vasculogenesis during the pulpal wound-healing process are not known. It has been proven that dental pulp has the ability to regenerate in teeth with incomplete apical closures [3,4]. There has been no report, however, on successful angiogenesis/vasculogenesis and pulp regeneration on the amputated pulp or disinfected root canals in teeth with complete apical closure without cell transplantation or without protein application. Endothelial progenitor cells (EPCs) home in to sites of neovascularization and differentiate into endothelial cells *in situ* [5]. This prompted us to explore cell therapy for angiogenesis/vasculogenesis and pulp regeneration to treat pulp injury. EPCs have been identified by cell-surface markers, AC133, CD34, VEGFR2, CXCR4 and c-Kit [5–7], and they have been shown to express endothelial markers, CD31 (PECAM) and CD146, following further differentiation [8]. We have recently isolated a distinct population of CD34$^+$, VEGFR2/Flk1$^+$, CD31$^-$/CD146$^-$ side population (SP) cells from porcine dental pulp that differentiate into endothelial cells *in vitro* and have been shown to enhance revascularization of hindlimb ischemia [9]. In the present study, we further examined the potential utility of this subfraction of cells from dog dental pulp for angiogenesis/vasculogenesis and pulp regeneration in a surgically amputated model of pulp injury.

Materials & methods

Cell isolation by flow cytometry

Canine primary pulp cells were separated from pulp tissues that had been extracted from one upper canine and then labeled with Hoechst 33342 (Sigma, St Louis, MO, USA), as previously described [10]. The isolated SP cells were cultured in EBM2 (Cambrex Bio Science, Walkersville, MA, USA) supplemented with IGF (Cambrex Bio Science), EGF (Cambrex Bio Science) and 10% fetal bovine serum (Invitrogen Corporation, Carlsbad, CA, USA). The SP cells at the second passage were further

10.2217/RME.09.5 © 2009 Future Medicine Ltd

subfractionated into $CD31^-$ and $CD31^+$ SP cells after labeling. The cells were then resuspended in HEPES buffer containing 2 µg/ml propidium iodide (Sigma). Analysis/sorting of cells was performed using a flow cytometer JSAN (Bay Bioscience, Kobe, Japan). Each cell fraction was plated into 35 mm collagen type I-coated dishes (Asahi Technoglass Corp., Funabashi, Japan) in EBM2 supplemented with suitable growth factors and 10% fetal bovine serum (Invitrogen Corporation) to maintain each phenotype. The medium was changed every 4–5 days. When the cells had reached 50–60% confluence, they were detached by incubation with 0.02% EDTA at 37°C for 10 min and subcultured at a 1:4 dilution.

The phenotypes of canine $CD31^-$ and $CD31^+$ SP cells were characterized at the second, third and sixth passage of culture. They were immunolabeled with mouse IgG1 negative control (AbD Serotec Ltd, Oxford, UK), mouse IgG1 negative control (fluorescein isothiocyanate; FITC, MCA928F, AbD Serotec), mouse IgG1 negative control (Alexa 647, MRC OX-34, AbD Serotec), and antibodies against CD146 (FITC; sc-18837, Santa Cruz, Biotech, Santa Cruz, CA, USA), CD14 (Alexa Flour 647, TuK4, AbD Serotec), CD34 (Allophycocyanin, APC, 1H6, R&D Systems, Inc., MN, USA) and CD105 (FITC; MEM-226, BioLegend, San Diego, CA, USA). The $CD31^-/CD146^-$ and $CD31^+/CD146^-$ SP cells were further isolated from $CD31^-$ and $CD31^+$ SP cells, respectively, at the third passage.

Endothelial cell differentiation *in vitro*

Multidishes with 96 wells were coated with 100 µl of Matrigel™ (BD Biosciences Pharmingen, San Jose, CA, USA). The $CD31^-/CD146^-$ and $CD31^+/CD146^-$ SP cells were seeded at the fourth passage (10^4 cells) on the Matrigel in EGM2 (EBM2 supplemented with VEGF, basic FGF, IGF, EGF, hydrocortisone, heparin, ascorbic acid and 2% fetal bovine serum) (Cambrex Bio Science). Network formation was observed after 12 h of cultivation.

Autogenous *in vivo* transplantation of stem cells on the amputated pulp

An experimental model of canine pulp partial removal [11] and transplantation of the $CD31^-/CD146^-$ or $CD31^+/CD146^-$ SP cells was established in adult dogs (Narc, Chiba, Japan). At the fourth passage, both of these populations, 2×10^5 cells in each, were cultured in pellets (cellular aggregates) with scaffold (collagen type I (Cellmatrix type IA, Nitta Gelatin, Osaka, Japan) and collagen type III (Cellmatrix type III, Nitta Gelatin) [1:1]) after DiI (Sigma) labeling at a final concentration of 4.7 µg/ml at 37°C for 15 min without serum. Under anesthesia with intraveneous sodium pentobarbital (Schering-Plough, Germany), surgical amputation was carried out approximately 1 mm under the cervical line by No. 018 round burr in three canine teeth per dog, and autogenous transplantation of the pellets on day 1 of cultivation was performed on the amputated pulp. The cavity was sealed with zinc-phosphate cement (Elite Cement, GC, Tokyo, Japan) and composite resin (Clearfil FII, Kuraray, Kurashiki, Japan) following treatment with a bonding agent (Clearfil Mega Bond, Kuraray). A total of 54 teeth from 18 dogs were used; six teeth transplanted with $CD31^-/CD146^-$ SP cells, six teeth transplanted with $CD31^+/CD146^-$ SP cells, two teeth without a pellet and four teeth with a scaffold only (without cells) were harvested for histology after 14 days. Six teeth, each transplanted with $CD31^-/CD146^-$ SP cells, $CD31^+/CD146^-$ SP cells and with a scaffold only (without cells) were harvested after 30 and 60 days. They were fixed in 4% paraformaldehyde (Nakarai Tesque, Kyoto, Japan) at 4°C overnight and embedded in paraffin wax (Sigma) after demineralization with 10% formic acid. The paraffin sections (5 µm in thickness) were morphologically examined after staining with hematoxylin and eosin.

Fluorescence microscopic images IX 71 (Olympus, Tokyo, Japan) in 5-µm thick paraffin sections of DiI-labeled transplanted cells were scanned into a computer and superimposed on to images of endothelial cell staining with anti-CD146 (sc-18837, Santa Cruz, CA, USA) and goat anti-mouse IgG-FITC (MP Biomedicals, LLC, Solon, OH, USA) to examine the migration and localization of transplanted cells.

For neuronal staining, 5-µm thick paraffin sections were deparaffinized, rehydrated and boiled with Protein Unmasking solution (Vector Laboratories, Burlingame, CA, USA), according to the manufacturer's instructions, to retrieve antigens. Sections were then blocked for endogenous peroxidase by incubating with peroxidase-blocking reagent (Dako Cytomation, Glostrup, Denmark) for 10 min. After incubation with 2.5% normal goat serum to block nonspecific binding, they were incubated with an antineurofilament antibody (ABC Laboratories, Ontario, Canada) (1:50) at 4°C overnight. Subsequently, peroxidase-conjugated secondary antibody